
# Airflow and energy analysis in geothermally heated conveyor drying of fishbone

Magnús Kári Ingvarsson

**Faculty of Industrial Engineering, Mechanical Engineering and Computer Science**
**University of Iceland**
**2014**

# AIRFLOW AND ENERGY ANALYSIS IN GEOTHERMALLY HEATED CONVEYOR DRYING OF FISHBONE

Magnús Kári Ingvarsson

30 ECTS thesis submitted in partial fulfillment of a
*Magister Scientiarum* degree in Mechanical Engineering

Advisors
Sigurjón Arason M.Sc., Professor, University of Iceland, Matís
Dr. Halldór Pálsson, Associate Professor, University of Iceland

Faculty Representative
Sveinn Víkingur Árnason

Faculty of Industrial Engineering, Mechanical Engineering and Computer Science
School of Engineering and Natural Sciences
University of Iceland
Reykjavik, June 2014

Airflow and energy analysis in geothermally heated conveyor drying of fishbone
30 ECTS thesis submitted in partial fulfillment of a Magister Scientiarum degree in Mechanical Engineering



Faculty of Industrial Engineering, Mechanical Engineering and Computer Science
School of Engineering and Natural Sciences
University of Iceland
VRII, Hjardarhagi 2-6
107, Reykjavik
Iceland

Telephone: (+354) 525-4000

Bibliographic information:
Magnús Kári Ingvarsson, 2014, Airflow and energy analysis in geothermally heated conveyor drying of fishbone, M.Sc. thesis, Faculty of Industrial Engineering, Mechanical Engineering and Computer Science , University of Iceland.

Printing: Háskólaprent, Fálkagata 2, 107 Reykjavík
Reykjavik, Iceland, June 2014

# Abstract

This study presents an investigation into airflow and energy aspects of a conveyor dryer in the drying of fishbone. The prototype of the dryer was designed by Sigurjón Arason and constructed in 1981, but since then, the size of the design has been scaled to build dryers of increased production capacity. The purpose of the study is to use measurements and methods of mass and energy balances to improve understanding and knowledge of the latest dryer built, so both the manufacturer of the dryer and its users can improve their product.

Measurements of airflow (flow rate, pressure, temperature and humidity) and product moisture content are made, and the measurement results are used to calculate key operating parameters. It is found that the adiabatic efficiency of the dryer is 50.5%, recycle ratio of exhaust air is 64% and the energy needed for evaporation of each kilogram of water from the product is 5500 kJ. The total energy consumption is evaluated as 919 kW for a production capacity of 800 kilograms raw material per hour. The measured humidity and pressure drop of air flowing through the dryer and other observations suggest that efficiency of the airflow can be improved. Measurements of product moisture content indicate that control of the drying process is far from optimal and with a change in procedures, there is an opportunity to at least double the production capacity.

# Útdráttur

Hér er tekin til skoðunar þurrkun fiskhryggja í færibandaþurrkara. Frumgerð þurrkarans var smíðuð árið 1981 eftir hönnun Sigurjóns Arasonar, en þurrkarinn nýtir jarðvarma til hitunar á lofti sem notað er til þurrkunarinnar. Litlar breytingar hafa verið gerðar a hönnun þurrkarans frá smiði frumgerðarinnar, aðrar en þær að stærð þurrkarans hefur verið sköluð upp til að auka afkastagetu. Tilgangur verkefnisins er að nota mælingar og aðferðir massa- og orkubókhalds til að auka skilning og þekkingu á virkni þurrkarans, svo bæði framleiðendur og notendur tækisins geti bætt sína framleiðsluvöru.

Mælingar eru gerðar á eiginleikum loftflæðis þurrkarans (flæði, þrýstingi, hita- og rakastigi) og vatnsinnihaldi afurðarinnar. Niðurstöður mælinga eru notaðar til að reikna helstu kennistærðir þurrkarans og fundið hefur verið að óvermin nýtni þurrkarans er 50,5%, hlutfallsleg hringrásun lofts er 64% og orkuþörf til að gufa upp hverju kílógrammi af vatni er 5500 kJ. Þá er heildar orkunotkun metin sem 919 kW fyrir framleiðslugetu sem samsvarar 800 kílógrömmum hráefnis á klukkustund. Niðurstöður benda til þess að nýtni loftflæðisins sé ábótavant hvað varðar þrýstifall og vatnsupptöku. Mælingar á vatnsinnihaldi vörunnar gefa til kynna að þurrkferlinu sé ekki rétt stýrt, verklagi sé ábótavant og tækifæri sé til þess að tvöfalda afköst.

# Contents

# List of Figures

# List of Tables

# Nomenclature

**Roman Symbols**

| | |
|---|---|
| $a_v$ | Specific surface, $1/\text{m}$ |
| $a_w$ | Water activity, dimensionless |
| $c_p$ | Specific heat, $\text{kJ}/(\text{kg} \cdot {}^\circ\text{C})$ |
| $D_p$ | Effective diameter, m |
| $G$ | Mass flow rate of dry air, kg/s |
| $h$ | Specific enthalpy, kJ/kg |
| $L$ | Thickness of product bed, m |
| $\dot{m}$ | Mass flow rate of (wet) product, $kg_{wet}/h$ |
| $M$ | Product moisture content (dry basis), $kg_{wet}/kg_{dry}$ |
| $P$ | Pressure, Pa |
| $q$ | Heat-transfer rate, kJ/s |
| $Q$ | Volumetric flow rate, $\text{m}^3/\text{s}$ |
| $r$ | Recycling ratio, dimensionless |
| Re | Reynolds number, dimensionless |
| $T$ | Temperature (dry bulb), °C |
| $v$ | Air velocity, m/s |
| $X$ | Product moisture content (wet weight basis), %wwb |
| $Y$ | Specific humidity, $\text{kg}_{\text{water}}/\text{kg}_{\text{dry air}}$ |

**Greek Symbols**

| | |
|---|---|
| $\eta$ | Efficiency, dimensionless |
| $\mu$ | Dynamic viscosity, $\mathrm{kg}/(\mathrm{s} \cdot \mathrm{m})$ |
| $\rho$ | Density, $\mathrm{kg}/\mathrm{m}^3$ |
| $\tau$ | Time, h |
| $\phi$ | Relative humidity, dimensionless |

**Subscripts**

| | |
|---|---|
| a | Air |
| i | Input (ambient conditions) |
| o | Output |
| s | Solids (product) |
| v | Vapor |
| w | Water |

# Acknowledgments

I would like to express my special appreciation and gratitude for the guidance and support of my advisors, Sigurjón Arason, professor at the Faculty of Food Science and Nutrition at the University of Iceland and chief engineer at Matís ltd., and Dr. Halldór Pálsson, associate professor at the faculty of Industrial Engineering, Mechanical Engineering and Computer Science at the University of Iceland.

I would like to thank Víkingur Þórir Víkingsson, production manager at Haustak ltd., for allowing me to measure the conveyor dryer at Haustak. I would also like to thank the monitoring specialists of the Icelandic Meteorological Office for letting me calibrate the measurement devices in their specialized facility.

It has been a privilege to work alongside as many brilliant, self-motivated people as I have, during my days at Matís ltd., and special thanks go to my colleagues there. Finally, I will always be grateful for the support and encouragement from my friends.

I acknowledge financial support from the Energy Research Fund, managed by National Power Company of Iceland, and the Icelandic Governmental Energy Fund.

# 1. Introduction

The tradition of drying seafood in Iceland dates back to the settlement, when drying was simply one of the few primitive techniques available for preserving food. The method for drying was to hang the raw material to dry under the open sky, but the inherent problem with this method is quality loss due to frost damage and insects laying their eggs in the product. For this reason, the drying has been moved indoors in the last decades, where the production is mechanized. In some cases geothermal energy is used to heat the air needed for drying. Indoor drying has multiple benefits over outdoor drying (Arason et al., 1982):

- Drying is possible throughout the year
- Drying time is shorter
- Higher yield of raw materials
- Optimized workflow and more predictable production rate
- Improved and more uniform product quality

In turn, demand and value has risen substantially in the years between 1982 to 2012, as figure 1.1 shows.

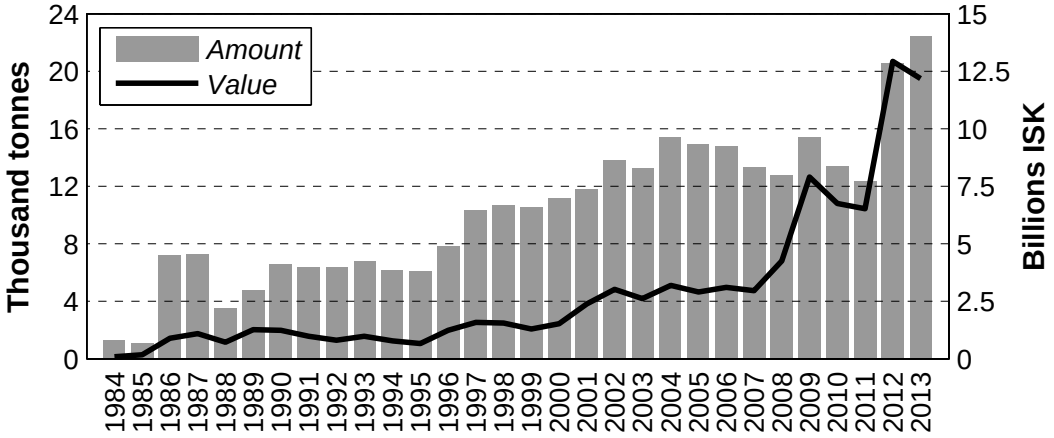


*Figure 1.1: Amount and value of dried fish byproducts exported from Iceland in the years 1984 to 2013 (Statistics Iceland, 2014).*

Information from figure 1.1, along with basic assumptions, can be used to estimate the annual energy consumption of the industry. Given that the average water content of the raw material and product is 80%wwb and 15%wwb respectively, it can be found that 85.000 tonnes of raw material must have been needed to produce the 20.000 tonnes of product in 2012. The energy needed to evaporate 65.000 tonnes of water at 20 °C is approximately 320 terajoules, given a 50% thermal efficiency of a typical cabinet dryer.

In effort to develop the production, a conveyor dryer was designed that would utilize geothermal energy to heat the air needed for effective and efficient drying (Arason, 2011). The conveyor dryer is well suited for drying seafood because it can handle a variety of raw materials, it fits the specific needs of the drying process, saves floor area and the production becomes continous (Poirier, 2006). The design enables recirculation of air from the dryer by partially mixing with air from the outside. This is done to control humidity and improve energy efficiency (Arason, 2013). Figure 1.2 shows the basic layout of such a dryer.

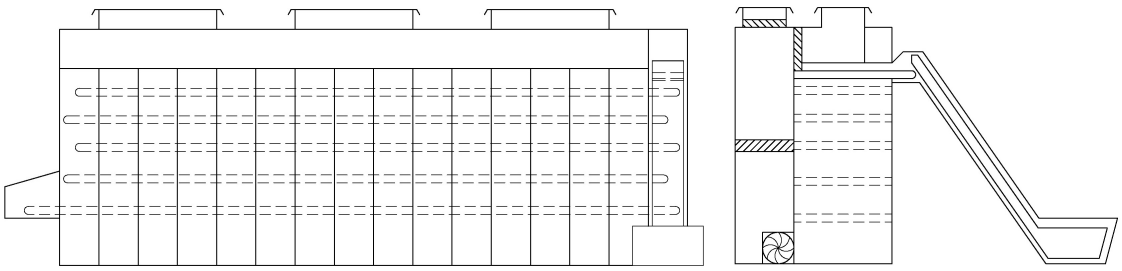

*Figure 1.2: Conveyor dryer layout, adapted from Arason (2011).*

Since the first dryer of this design was built in 1981, more than 6 dryers have been built with only minor modifications to the design, although their size has been scaled to fit larger production capacities. Unfortunately, the original process design does not scale in the same way as the geometry and there are indicators that insufficient understanding of the heat and mass transfer processes in the latest dryers has lead to poor product handling, nonuniform product quality and wasted energy (Arason, 2013).

Most countries do not have geothermal energy sources available for drying and may need to exploit other, more expensive, sources for heating air, such as coal, oil or electricity. In addition, requirements for drying seafood specify an allowable humidity range of the air used for drying, and therefore it is more difficult to recirculate hot air in a humid climate. If cost of heating is high and potential for recirculation is minimal, operators will be tempted to increase energy efficiency by raising air temperature which will increase the rate of drying, even though product quality will likely suffer. With better control of the airflow, the product might be dryed at lower temperatures with acceptable efficiency (Arason, 2013).

There is a clear gap in literature when it comes to drying seafood in a conveyor dryer and even more so if the topic is more specific. The know-how within the Icelandic industry is present, but latest published research on the topic is at least a decade old (Arason, 2001). Also, there is need for improved knowledge of the energy efficiency of the design, so that it may utilize other heat sorces than geothermal. This gives a reason for an investigation.

The main objective of this study is to use measurements from a conveyor dryer to set up moisture and energy balances, analyze the airflow and construct a model for the process of drying fishbones. The results will be used to shed light on the energy aspects of the dryer in order to enable both manufacturers and operators of such dryers to improve their product. The purpose is to improve insight and knowledge of energy aspects the equipment. Another result of the study will be a confirmation of the performance of the equipment.

The content of this thesis is presented in the following order:

- Chapter 2 presents an introductory discussion of the concepts of drying seafood, an explanation of the conveyor dryer and finally how mass and energy balances can be applied to analyse it.
- Chapter 3 describes the methods and materials used for aquiring data. Limitations to the survey are explained and and how some of the encountered challanges are met.
- Chapter 4 presents results of measurements and analysis thereof, including immidiate conclusions. The chapter is divided into four sections: air pressure and flowrate, temperature and humidity, product flow and finally balance calculations.
- Chapter 5 presents a summary of conclusions that may be drawn from the results.

# 2. Background

To provide context for the work presented in this thesis, the chapter reviews the philosophy and technology of drying seafood, with emphasis on conveyor dryers. Following an introduction to the concepts of drying, is a discussion about the process of drying seafood. The workings of a conveyor dryer is explained and lastly the theory used for analysing the process.

## 2.1. Concepts of drying seafood

Drying seafood is the process of thermally removing water from the product. Water in seafood can be either intra- or extracellular, it can be found in chemical compounds, in solution or trapped inside microstructures. The portion of water within a product which exerts a vapor pressure less than that of pure water is called bound water and the water in excess of bound water is called unbound water, which can be removed by drying (Arason et al., 1982; Rahman, 2006).

Moisture content is usually expressed in terms of mass rather than volume, as the volume of a material being dried may change in the process (Keey, 1972). In this thesis, moisture content of the product wil either be expressed in terms of the whole mass (wet basis) and denoted by $X$, or in terms of bone dry solid in which case it will be denoted by $M$.

Most seafood is very delicate and can easily be spoiled by microbes, chemical reactions, physical deterioration and nutritoinal loss. The chemical potential of water in the product will determine the rate of quality loss, as water will take part in reactions and act as a medium for substances that will increase the rate of spoilage (Rahman, 2007). Activity is a concept from chemical thermodynamics which can be used as a measure for the chemical potential of water and is then called water activity, denoted by $a_w$ (Zeuthen and Bøgh-Sørensen, 2003).

For thermodynamic equilibrium at atmospheric pressure, water activity can be

defined by

$$a_w = \frac{p_w}{p_0}$$

where $p_w$ is vapor pressure of water in equilibrium with the product and $p_0$ is the vapor pressure of pure water at the same temperature (Zeuthen and Bøgh-Sørensen, 2003). The general effects of water activity on the relative rate of quality loss in food products can be seen in figure 2.1. The purpose of drying is to reduce $a_w$, so bacteria, yeasts and molds can not grow and spoil the food. The critical water activity for fishbones and fish heads is 0.4 (Arason, 2011).

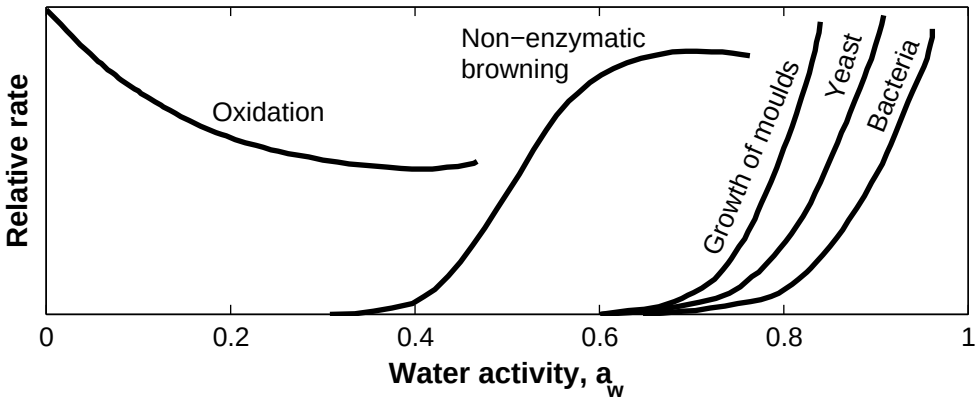


*Figure 2.1: Relative rate of spoiling as a function of water activity. Adapted from (Chen and Mujumdar, 2009).*

When internal vapor pressure of water in the product is equal to the outside vapor pressure, the product is said to be in equilibrium with its surroundings. During equilibrium the relative humidity of the surrounding air can be related to the water activity (Chen and Mujumdar, 2009).

$$\phi = 100\% \cdot a_w$$

At this stage, the product is stable and moisture content is constant and the relative humidity of the air and moisture content of the product are respectively referred to as equilibrium relative humidity and equilibrium moisture content. There is a specific relationship between the equilibrium relative humidity and equilibrium moisture content for variable temperature that is called a water sorption isotherm, but sorption isotherms are characteristic for different products. As the product will always seek to be in equilibrium with its surroundings, a sorption isotherm can be used to predict the terminal moisture content of a product if the ambient conditions ar known (Mujumdar, 2006).

There are only a few sources for research on sorption isotherms for (salted) codfish in literature (Arason et al., 1982; Boeri et al., 2013; Van Arsdel et al., 1973), but to the authors best knowledge there are none available for fishbone or fish heads. Final

moisture content of products is an agreement between producer and customer, usually 12-15% for stockfish, fishbone and fish heads (Arason, 2011).

Drying can be seen as two processes that happen concurrently and rate of drying is determined by the rate at which these two processes proceed (Mujumdar, 2006):

1. *External process*: Energy is transferred from the environment to the product to evaporate moisture from the surface. This process depends on the external conditions of temperature, humidity, pressure, flow of air and area exposed to the environment.
2. *Internal process*: Moisture is transported via diffusion and capillary action to the surface of the product due to difference in concentration of dissolved substances, where it evaporates due to process 1.

Fresh fish has high moisture content (more than 50% wet basis) and therefore demonstrates two distinct drying periods: a *period of constant drying rate*, where the moisture closest to the surface evaporates and external conditions (process 1 above) is the only limiting factor, and a *period of falling drying rate* when the internal process becomes the bottleneck (Arason et al., 1982). The change from a constant drying rate to a falling rate occurs when a critical moisture content is reached. An ideal drying curve is shown in figure 2.2, where the critical moisture content and equilibrium moisture content are denoted by $M_c$ and $M_{eq}$ respectively.

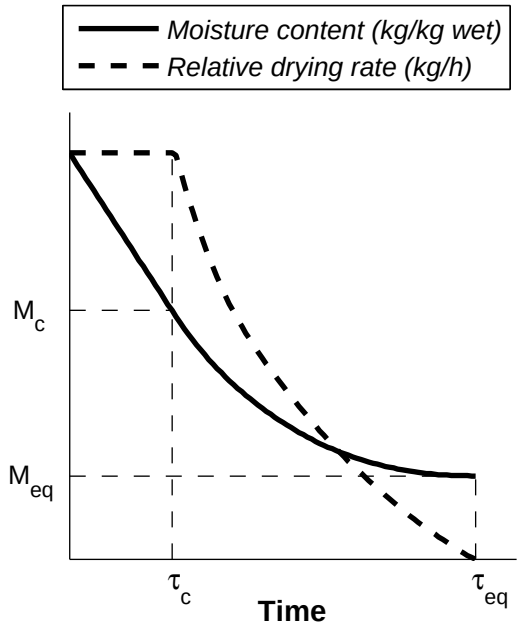


*Figure 2.2: Ideal drying curve for high-moisture food, such as fish.*

The drying process is usually split into two stages: primary and secondary drying. Primary drying is conducted in a conveyor dryer during period of constant drying

rate, or until the product reaches critical moisture content (usually 30-55%wwb). Secondary drying is carried out in special containers (see figure 2.3) during the period of falling drying rate, until the moisture content of the product has reached 11-18%wwb (depending on the final product specification). The main benefit of this division is that relatively larger quantities of product can be placed in secondary drying due to difference in drying rate. In addition, initial and operational cost of secondary drying is much lower than that of primary drying (Arason, 2001).

*Figure 2.3: Drying containers used in secondary drying (Photo: Lárus Karl Ingason).*

Three parameters of the external conditions dictate drying rate throughout the period of constant rate above others, those are temperature, humidity and velocity of the drying air. Optimal drying rate is effectively the highest drying rate that will not result in a loss of quality. In other words, quality standards form the criteria for the external conditions. If drying is too rapid, a layer of compressed cells will form at the surface of the product (shelling). This layer will hinder transportation of moisture to the surface and prevent evaporation. Quality loss during drying can also be due to protein folding and browning. (Arason, 2011).

The rate of evaporation from the surface is determined by the rate of diffusion of water vapor through a stationary film of air surrounding the product. The rate of diffusion will increase with increasing air velocity, as a result of decreased thickness of the film (Lewis, 1921). Research has shown that the suggested air velocity for drying fish is in the range of 1.5-3.0 m/s during primary drying, to prevent shelling (Arason, 2001; Arason and Árnason, 1992; Arason et al., 1982). For a similar reason, the recommended range for relative humidity is 20-50% to prevent shelling (Arason, 2001, 2011; Arason and Árnason, 1992). Folding of fish protein will begin at temperatures above 25 °C (Arason et al., 1982), and research indicates that the recommended temperature is in the range of 18-25 °C (Arason and Árnason, 1992).

To increase production capacity, it is appropriate to put effort into optimization of the drying rate, taking into account external conditions along with other variables and criteria. For this reason, it is no surprise that modeling of drying curves plays an important role in the literature of drying and many different models exist for different types of processes. For instance, a list of models for thin layer drying is shown in table 2.1, most of which include exponential decay.

*Table 2.1: Various mathematical models for drying curves for thin layer drying.*

| **Model name** | **Moisture content** | **References** |
|---|---|---|
| Lewis | $\exp(-k\tau)$ | (Bruce, 1985) |
| Page | $\exp(-k\tau^n)$ | (Page, 1949) |
| Modified Page | $\exp(-k\tau)^n$ | (White et al., 1981) |
| Henderson and Pabis | $a \cdot \exp(-k\tau)$ | (Henderson and Pabis, 1961) |
| Exponential | $a \cdot \exp(-k\tau) + c$ | (Toğrul and Pehlivan, 2002) |
| Two-term model | $a \cdot \exp(-k_0\tau) + b \cdot exp(-k_1\tau)$ | (Henderson, 1974) |
| Wang and Singh | $1 + a\tau + b\tau^2$ | (Wang and Singh, 1978) |
| Simplified Fick's diffusion | $a \cdot \exp(-c(\tau/L^2)$ | (Diamante and Munro, 1991) |
| Modified Page equation-II | $\exp(-c(\tau/L^2)^n)$ | (Diamante and Munro, 1991) |

In this study, a exponential model will be used to model moisture content of fishbone during drying.

$$M(\tau) = a \cdot \exp(-k\tau) + c \tag{2.1}$$

Using a exponential function to model the moisture content seems intuitive. Each term of the model describes some characteristic of the process: $a$ compensates for the inital moisture content, $k$ is a shape factor and $c$ represents the terminal moisture content.

## 2.2. The conveyor dryer

This study is focused on a conveyor dryer operated by the seafood drying company Haustak. Haustak is a subsidiary of two Icelandic fishing companies, Vísir and Þorbjörn, and it is the largest seafood drying company in Iceland. Haustak is situated on Reykjanes peninsula (63°49'38.3"N, 22°41'44.6"W), a half kilometre south of Reykjanes power plant which supplies the geothermal brine used as an energy source for drying.

The dryer was originally designed for blue whiting and capelin, but today it is predominantly used for fish heads and bones. So despite a simple design, the conveyor dryer is versatile and suitable for drying varied products. Table 2.2 shows the product range for the dryer.

*Table 2.2: Haustak conveyor dryer product range.*

| | Heads | Chops | Bones | Stockfish | Whole |
|---|---|---|---|---|---|
| **Haddock** | x | x | x | | |
| **Cod** | x | x | x | | |
| **Skate** | | x | | | x |
| **Ling** | x | x | x | x | |
| **Saithe** | x | | x | | |
| **Tusk** | x | x | x | x | |

The dryer has a five stage configuration. Five conveyor belts are arranged one above the other, running in opposite directions. Product is loaded onto the top belt and it cascades down to belts below. At the end of each belt is a drum which breaks up clumps of product that have formed after sticking together during drying. The dryer enclosure is constructed of a steel frame, with polyethylene panels on the sides and steel shutters at the ends for accessibility. The belts are approximately 18.1 m long and 2.8 m wide. Total height of the dryer is roughly 8 meters.

Hot air is forced up through the product bed while the product travels through the dryer. Blowers draw air from the outside through a heating element and then compress it to create a pressure difference across the perforated conveyor belts so that the air will flow through them. Air control vanes are installed to control how much fresh air is used and how much air is recycled. Direction of the airstream is opposite to the flow of product (counter-flow). This is an essential feature of the design, because it makes drying rate more even at different stages and prevents excessive rate of drying on the top belts, which would lead to loss of quality (Arason, 2011). Figure 2.4 shows a cross section of the dryer with the critical components of it marked.

The intended drying time for fishbone is 30 hours in primary drying, or until the product has reached 50-60% of its original weight (Arason and Árnason, 1992; Arason et al., 1982). At Haustak, it is standard practice to load a fresh bed of product onto the entire top conveyor at once and let it dry until it is time to load a whole new bed. This semi-continous method of operation is meant to integrate with the rest of the process and ensure a uniform product at a low unit cost (Keey, 1972). The operator of the dryer will strive to maintain a consistent total drying time and has relative speed of the belts configured to control the thickness of the bed on each belt. However, as the dryer is only run during 8 hour long daytime shifts, the estimation and prediction of effective drying time of the product at each stage can become judgemental.

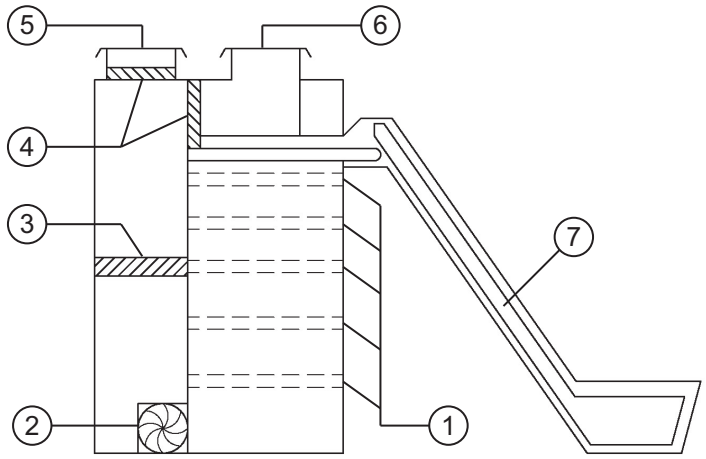


*Figure 2.4: Conveyor dryer layout and critical components. 1) Conveyor belts, 2) blowers, 3) heat element, 4) air control vanes, 5) air inlet, 6) air outlet, 7) product infeed conveyor.*

## 2.3. Mass and energy balances

The dryer is an open system where mass and energy are transfered in form of hot air and wet product. The drying process is effectively continuous and a steady state is assumed where all conditions are taken to be invariant with time. Based on this assumption, continuity equations of mass and energy can be applied (White, 2011), which implies that all mass and energy entering the dryer is equal to that leaving or accumulating inside.

Mass and energy balances may be applied to each conveyor in series to analyze the process as a whole. Measurements of airflow conditions and product stream at intermediate stages can be used for this purpose. Figure 2.5 shows measurable quantities used in balance calculations.

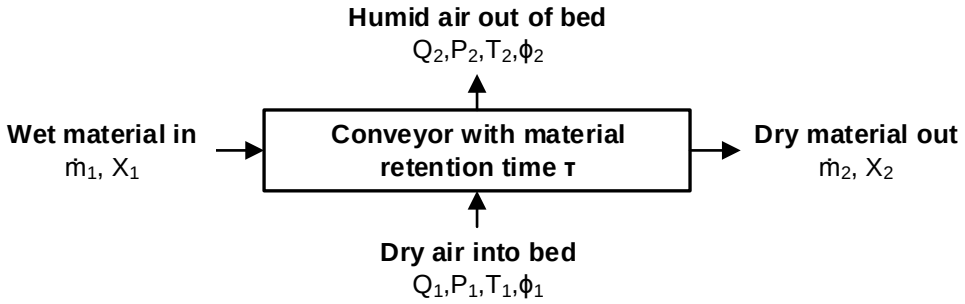


*Figure 2.5: Moisture and energy balance (Keey, 1972).*

All moisture removed from product inside the dryer must evaporate into the airstream (Keey, 1972). Hence, a mass balance across the whole dryer can be

written as

$$\dot{m}_i X_i - \dot{m}_o X_o = G(Y_o - Y_i) \tag{2.2}$$

where $\dot{m}$ is mass flow of product and $G$ is the mass flow of dry air. Subscript $i$ refers to an inlet position (ambient conditions) to the dryer and subscript $o$ to an outlet, hence counter-flow operation. By separating inputs and outputs the balance can be rearranged:

$$\dot{m}_i X_i + GY_i = \dot{m}_o X_o + GY_o \tag{2.3}$$

To increase thermal efficiency, some humid air may be recycled from the outlet. If $r$ denotes the recycle ratio, equal to the mass of dry air recycled per unit mass of dry air flowing through the dryer, the mass balance becomes (Keey, 1972, 1991):

$$\dot{m}_i X_i + (1-r)GY_i + rGY_o^+ = \dot{m}_o X_o + GY_o^+ \tag{2.4}$$

Let

$$(1-r)GY_i + rGY_o^+ = GY_M$$

and since mass is conserved, it follows that:

$$r = \frac{Y_M - Y_i}{Y_o^+ - Y_i} \tag{2.5}$$

Like mass, energy is conserved, so the net heat flow into the dryer and the net work done (e.g. blower work) is equal to the difference in enthalpy of the input and output streams. Energy in other forms, such as kinetic and potential energies, are relatively small and are ignored (Keey, 1972). The absolute minimum amount of heat necessary to achieve drying (to turn each kilogram of moisture into vapor) is equal to the latent heat of evaporation (Kemp, 2012).

$$q_{H,min} = (\dot{m}_i X_i - \dot{m}_o X_o)\Delta h_w \tag{2.6}$$

In practice, drying consumes substantially more energy than the latent heat of evaporation. With inspiration from Kemp (2012) and Keey (1972), the rate of heat supply through the heat exchanger (excluding losses) is written as

$$\begin{aligned} q_H &= (1-r)Gc_{p_a}(T_h - T_i) + rGc_{p_a}(T_h - T_o) \\ &= Gc_{p_a}((1-r)(T_h - T_i) + r(T_h - T_o)) \end{aligned} \tag{2.7}$$

where $T_h$ denotes temperature of the heated air entering the dryer and $T_i$ remains the temperature of the ambient air supply. A heat balance presented by Kemp and Gardiner, 2001 equals heat given up by air inside the dryer to the sum of latent heat of evaporation, sensible heating of product and heat losses.

$$Gc_{p_a}(T_h - T_o) = (\dot{m}_i X_i - \dot{m}_o X_o)\Delta h_w + q_s + q_{loss} \tag{2.8}$$

Combining equations (2.7) and (2.8) yields the overall heat balance:

$$q_H = \frac{(1-r)(T_h - T_i) + r(T_h - T_o)}{(T_h - T_o)}[(\dot{m}_i X_i - \dot{m}_o X_o)\Delta h_w + q_s + q_{loss}] \tag{2.9}$$

One way of evaluating the energy balance is taking the dryer to be adiabatic, where it has no exchange of heat with the surroundings (Keey, 1972; Kemp, 2012). In this case, the latent heat of evaporation corresponds to the temperature drop of the air, and the heat supplied corresponds to the temperature rise of the air. The adiabatic drying efficiency is then defined as:

$$\eta = \frac{(T_h - T_o)}{(1-r)(T_h - T_i) + r(T_h - T_o)} \tag{2.10}$$

The numerator represents the temperature difference which corresponds to useful heat of evaporation and is therefore an important factor of the efficiency. The recycling ratio is also an important factor of the efficiency. In the impossible scenario where all the air is recycled, the adiabatic efficency is 100 %. On the other hand, if no air is recycled, the adiabatic efficency will take a familiar form, $\eta = (T_h - T_o)/(T_h - T_i)$. A comparison of the actual, non-adiabatic, efficiency and the adiabatic efficiency can be used to estimate losses.

Kemp (2012) describes different types of losses in drying. Main sources of losses are exhaust heat losses and losses due to exhaust temperatures above dewpoint temperature. Ideally, the drying air would cool adiabatically while absorbing moisture from the product until reaching saturation and/or equilibrium with the product. These losses arise from inefficiency in the rate of heat transfer between drying air and product. Other sources of losses may be due to heat losses from the dryer body (typically 5-10%) and heating of the product.

The product may be heated during period of falling drying rate as bound moisture is removed. If heat is supplied in excess of latent heat of evaporation, sensible heating of product will occur. In this case, energy is being used for heating the product rather than for evaporation (Kemp, 2012). This causes outlet humidity to fall for the same exhaust temperature and reduces efficiency. Sensible heating of product is calculated by

$$q_s = \dot{m}_i h_i - \dot{m}_o h_o$$

in which the enthalpy of the product is estimated using

$$h = (c_p)_s T_s$$

where $(c_p)_s$ and $T_s$ represent the specific heat capacity and temperature of the product respectively. Specific heat capacity of the product is approximated with a linear combination of specific heat capacities of the components of the product (mostly water and protein) at any time, by weight. Table 2.3 shows a a typical

material balance for fishbone at three different stages in production. The mass-balance shows how the proportions of the components and specific heat capacity of each component is shown in table 2.4.

*Table 2.3: A sample of material balance for primary and secondary drying of fishbone (Arason, 2011).*

| Ingredients | Raw Material | | Semi-dried | | Fully dried | |
|---|---|---|---|---|---|---|
| | % | kg | % | kg | % | kg |
| **Water** | 79 | 79.0 | 55 | 25.7 | 17 | 4.3 |
| **Protein** | 18.7 | 18.7 | 40 | 18.7 | 74 | 18.7 |
| **Minerals** | 1.9 | 1.9 | 4 | 1.9 | 7 | 1.9 |
| **Fat** | 0.4 | 0.4 | 1 | 0.4 | 1 | 0.4 |
| **Wet** | 79 | 79.0 | 55 | 25.7 | 17 | 4.3 |
| **Solid** | 21 | 21.0 | 45 | 21.0 | 83 | 21.0 |
| **Total** | 100 | 100 | 100 | 46.7 | 100 | 25.3 |

*Table 2.4: Specific heat capacity of food components at 20 °C.*

| Component | Specific heat capacity kJ/(kg · °C) |
|---|---|
| Water | 4.18[†] |
| Protein | 1.55[‡] |
| Minerals | 0.84[‡] |
| Fat | 1.67[‡] |

[†]Holman (2010)
[‡]Hallström et al. (1988)

## 2.4. Airflow and airflow modeling

For decades the topic of flow through packed beds has been a subject of research within different branches of engineering and science. Studies have focused on theoretical modeling, experiments and numerical methods. Leva et al. (1951) provide a literature survey and a thorough discussion of the topic in general. More recent studies have put numerical methods to use for advancing modeling accuracy in regard of particle geometry, particle and bulk density, bed porosity and so forth (Prado and Sartori, 2008, 2011).

The flow of air through the dryer is restricted by the belts and the product bed on top of them. It is relatively straightforward to measure airflow pressure drop and Poirier (2006) states that testing or previous experience will never be replaced by theoretical modeling; that effects experienced within conveyor dryers are very

difficult to predict. He points out that permeability will not change linearly with depth and that effects such as product clumping are too difficult to predict with a theoretical model. Another challenge to modeling pressure drop is the fact that characteristics of the product bed will change as the drying progresses. However, despite these difficulties, it is hard to deny the value of using theory, if not only to compare it to the measurements and using it to gain better understanding of the airflow.

In 1952, an article on fluid flow through packed columns was published (Ergun, 1952). The author found that pressure losses are caused by simultaneous kinetic an viscous energy losses, and proposed an equation applicable to all types of flow. The equation expresses the friction factor and pressure drop in packed bed columns as a function of the Reynolds number:

$$f_p = \frac{150}{\mathrm{Re}} + 1.75$$

where

$$f_p = \frac{\Delta P}{L}\frac{D_p}{\rho v^2}$$

and

$$\mathrm{Re} = \frac{D_p v \rho}{(1-\epsilon)\mu}$$

Solving for $\Delta P$ gives

$$\Delta P = 150\frac{\mu v L}{D_p^2}\frac{(1-\epsilon)^2}{\epsilon^3} + 1.75\frac{\rho v^2 L}{D_p}\frac{(1-\epsilon)}{\epsilon^3} \tag{2.11}$$

Here, $\epsilon$ represents the void fraction, defined by

$$\epsilon = \frac{\text{volume of voids in bed}}{\text{total volume of bed}}$$

The effective particle diameter of a nonspherical particle is defined as

$$D_p = \frac{6}{a_v}$$

where $a_v$ represents specific surface of the particle, which is equal to the ratio between suface area of the particle to its volume.

In this study, equation (2.11) will be used to predict the pressure drop along the thickness of the product bed after measuring the air velocity into the bed and estimating the size of the product. For sake of simplicity, fishbone will be modeled as thin plates. Viscosity and density of the air are found using psychrometric charts. A description of how parameters of the equation are attained is described in the next chapter.

# 3. Measurements

This chapter will discuss design of experiments and describe the methods used to obtain essential data for a practical analysis of the process. Emphasis is placed on use of measurements that conform with the objectives in as many ways as possible. Before measurements can be carried out, a number of practical issues must be recognized because they significantly shape the outcome of the research.

The initial step of performing measurements is knowing which parameters are needed for the study. For a basic psychrometric description of air three parameters are needed, e.g. dry-bulb temperature, relative humidity and pressure. With these three parameters known, one can determine moisture ratio, specific enthalpy and specific volume of humid air. CoolProp is an open-source, cross-platform, free property database written in C++ that includes humid air properties (Bell et al., 2014). This database can be used through many programming languages, for example Matlab or Python, and is therefore a convenient tool for analyzing and modeling drying processes.

A barrier when measuring a conveyor dryer is limited accessibility. The dryer itself is closed to prevent hot air from escaping and therefore it is difficult to insert any sort of instrument. One option would be to open a hatch on the short side of the dryer and crawl inside to attach an instrument to the dryer. This is hardly practical because the dryer would first need to be emptied to insert an instrument and then again to retrieve it. The second and preferred option is to drill a small hole in the side of the dryer such that a slim, handheld instrument may be inserted.

Five holes would be needed in order to make measurements between each pair of adjacent belts and beneath the bottom belt, but the operator of the dryer is concerned about the appearance of the equipment and will only allow for two holes to be drilled into the dryer from within the blower compartment. One hole is drilled beneath the bottom belt and another beneath the middle belt, both 3 centimeters in diamater. Holes are closed as neatly as possible using a PVC pipe fitting and a lid, as shown in figure 3.1.

The zones accessible for making measurements are denoted in figure 3.2. Since the holes are drilled into the dryer from the blower compartment (zone 2), differential pressure measurements are impossible in most situations because of the layout of

*Figure 3.1: Marked with red is a pipe fitting used to close a hole drilled into the dryer in order to insert measurement probes.*

the dryer. In any case, a manometer is likely not a feasible method for measuring pressure differences over long distances, in a turbulent environment to a precision of 10 Pa. Using a handheld device to make absolute pressure measurements is seen as a more flexible and accurate method for finding pressure differences in this scenario.

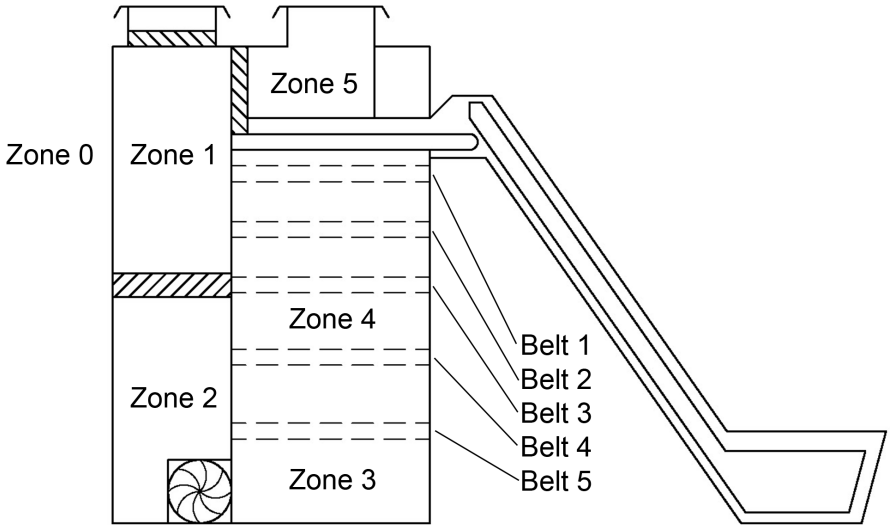


*Figure 3.2: Numbering of zones and belts.*

No instruments at a reasonable cost have been found in the market that fit the physical format required or otherwise fulfill the specific needs of the study. For this reason, a customized intstrument is designed and built to offer reliability, repeatability and accuracy at low cost while measuring temperature, humidity and pressure. A description of the instrument, which is entirely based on open source hardware and free software can be found in appendix A.

The main drawback of using a single handheld instrument, is that simultaneous measurements are not possible. To compensate for this drawback, a number of measurements are made in each zone (never fewer than three) and an effort is made to make as many measurements within a given timeframe as possible. Each measurement of temperature, humidity and pressure lasts for two minutes with a sample rate of roughly 1 Hz.

Having access to measure only three out of six intermediate stages inside the dryer itself (zones 3, 4 & 5) would require simplifications of process analysis and modeling. However, knowing the product moisture content at the beginning and end of each belt of the dryer can be used to complement airflow measurements for it can be used to estimate how much water the airflow takes up from the product at different stages during drying. By measuring the change in product moisture content on each belt, an opportunity is created to equate the rate of evaporation from the product to the moisture uptake of the air. This can also be used to approximate state of the airflow where no actual airflow measurements are possible.

The method used for determining the moisture content is to completely evaporate the unbound moisture from a sample. Sample material is prepared by cutting the material into small pieces of 4-5 cm in length and placing a sample of known mass (40-60 grams) into a dry and weighed glass container, which is put into an oven and dried at 110 °C for roughly 24 hours. Once the sample has been allowed to cool down in a desiccator its mass is measured at ambient temperature. While this method is relatively straightforward, it offers an estimated accuracy of $\pm 1.0\%$, which is sufficient for the purpose of this analysis. Figure 3.3 shows the weighing of samples before drying.


*Figure 3.3: Weighing of samples for determining moisture content of the product.*

A handheld anemometer, a model Testo 452 (with probe 0635-6045), is used for measuring air speed at various locations around the dryer (Testo AG, N.d.). The anemometer is used for measuring velocity of the air flowing into the belts and

the velocity of air flowing into blowers so that the total flow rate of air can be estimated. Readings are instantaneos and are logged manually.

Apart from measuring product moisture content and airflow conditions, other observations are also made. Temperature of the product at intermediate stages is measured and logged. Make and model of blowers is noted so their specification sheet can found. The geometry of the dryer and belts are sized using a measuring tape. A supervisory control and data acquisition system is used to control and monitor the dryer; miscellaneous information is gathered from this system, such as control parameters, temperatures in the system and more. Finally, a short interview is taken with the operator for general questions about the dryer (operation, production, problems and more).

# 4. Results and discussion

Measurement results provide a range of possibilities for different analyses that can shed light on workings of the dryer. The theory presented in the previous background chapter is used to realize those possibilities. Most elements of this study can be approached from different perspectives, e.g. using measurements, theory or production experience. The chosen approach is to generally put trust in the measurements without challenging other information, but instead try to seek explanation of how the different perspectives can coexist.

## 4.1. Air pressure and flowrate

Pressure measurements show stable pressures in all zones. Figure 4.1 exhibits a five minute long pressure measurement from beneath belt 5 (zone 3), in which pressure range is 32 Pa for raw readings and 14 Pa after filtering with a 30 second moving average. Stable pressure readings are a positive indication, suggesting using single pressure measurements is a sufficiently accurate method.

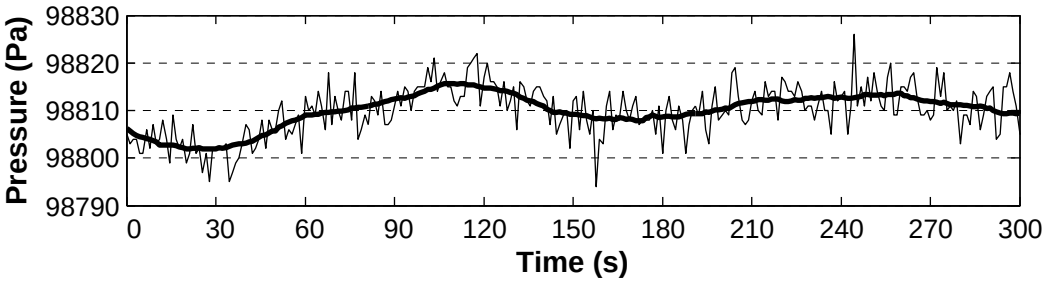


*Figure 4.1: Sample of a pressure measurement from zone 3.*

Results of pressure measurements are presented in figure 4.2. Total pressure difference, contributed by blowers, is equal to the sum of pressure drop through the heating element (decrease from zone 1 to 2) and pressure head (increase from zone 2 to 3). Therefore, total pressure difference through the whole dryer is in range of 350 to 470 pascal.

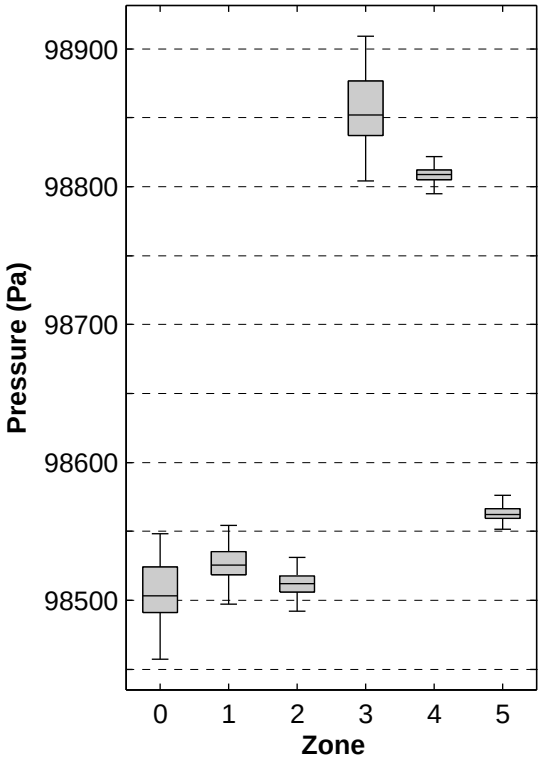


*Figure 4.2: Unfiltered pressure measurements. Center line on each box indicates median value and edges of boxes mark 25th and 75th percentiles. Extreme values, excluding outliers, are represented by extended threads.*

Measured air velocity at blower suction inlet is $21.5 \pm 0.5\,\mathrm{m/s}$. For a blower inlet diameter of 805 mm, this is equivalent to a volumetric flow rate of approximately $10.95 \pm 0.25\,\mathrm{m^3/s}$ for each blower, or a total of $65.6 \pm 1.5\,\mathrm{m^3/s}$ for six blowers. Area of each belt is $2.8\,\mathrm{m} \cdot 18.1\,\mathrm{m} = 50.7\,\mathrm{m^2}$, so mean velocity of air into a belt would be

$$\bar{v} = \frac{Q_{blowers}}{A_{belt}} = \frac{65.6 \pm 1.5\,\mathrm{m^3/s}}{50.7\,\mathrm{m^2}} = 1.30 \pm 0.03\,\mathrm{m/s}$$

A substantial uncertainty is inevitably involved in this measurement. An error of $0.1\,\mathrm{m/s}$ in air velocity measurement will amount to an uncertainty of $1100\,\mathrm{m^3/h}$ for six blowers.

There is a way to simultaneosly verify measurements of pressure and flow rate by checking whether they are in accordance with rotational speed of blowers. Six centrifugal blowers, manufactured by Italian company Dynair, are installed in the dryer. Specifications are shown in table 4.1. Relationship between pressure contribution and flowrate for a given rotational speed of a blower is described by characteristical performance curves, found in a specification sheet (Dynair, 2014).

*Table 4.1: Blower specifications (Dynair, 2014)*

| | |
|---|---|
| Manufacturer | Dynair Industrial Ventilation |
| Blower model & type | PR-L 804 T RD |
| Year of manufacture | 2006 |
| Suction inlet diameter | 805mm |
| Power rating | 22kW |
| Number of poles | 6 |
| Volts / Phases / Frequency | 400-690 / 3 / 50 |
| Rated RPM | 1400 |

A readout from a system control panel indicates that a variable frequency drive for the blowers is set at 40Hz. Assuming low slip in induction motors driving the blowers, speed of the motor is taken to be approximately proportional to power supply frequency (Rakesh, 2003). Given a rated speed of 1.400 revolutions per minute for a 50 Hz power supply, the speed should be around 1.120rpm at 40 Hz.

Investigation of characteristical curves shows that pressure increase is in the range of 330 to 450 pascals for the flow rate and rotational speed above. Efficiency of the blower drops below 51% in this range, but optimal efficiency is 81% (Dynair, 2014). A basic approach to airflow design is to install a somewhat oversized blower and then turn it down, using a variable frequency drive, so that it meets the required specification with sufficient efficiency. In this case however, the low efficiency shows that the blower is clearly intended for higher efficiency at higher pressures. This is consistent with pressure measurements and raises the suspicion that pressure drop through the dryer may not be the same as it has been designed to be.

It is worth considering why the pressure drop seems to be lower than what might have been expected, given the size of the blowers and their low efficiency. As mentioned before, there is a gap at the end of each belt, where the product falls onto the belt below. This gap, which is 1 m wide and 2.8 m long, is shown in figure 4.3. Velocity of air streaming through the gap by belt 1 was measured to be 8 m/s, which is equivalent to more than a fair share of the total volumetric flow. This raises the question, whether some portion of the airflow might be zigzagging through the dryer, flowing through the gaps at the ends.

Another potential explanation for a low pressure drop, might be apparent gaps in the product bed as shown in figure 4.4. If lights are turned on at one side of the dryer, the product will cast a shadow onto the wall of the dryer on the opposite side and reveal gaps in the product bed. Uneven loading of the product onto the belt could be a cause for irreglurities in the the airflow.

A factor that is known to affect pressure drop inside the dryer is the opening ratio

*Figure 4.3: A gap at the end of a conveyor belt inside the dryer where product falls onto the next belt. Also shown in this photo is the breaker drum.*

*Figure 4.4: Gaps in the product bed on belts 1 and 5.*

of the conveyor belt, i.e. ratio of area of the belt open for airflow to a unit area of belt. The photographs in figure 4.5 depict two samples of belt from the dryer and how product residuals have accumulated in the belt and reduced its opening. Analysis of photographs taken of the belt indicate that the opening of a clean belt is approximately 0.35, but for samples A and B in figure 4.5 the opening is 0.27 and 0.2 respectively.

Ashworth Brothers Incorporated, a pioneering conveyor belt manufacturer, has commissioned independent testing laboratries to conduct comparative air flow tests and quantify air pressure drop of their plastic belts. Ashworth has been contacted for results of these tests and with their kind permission an excerpt is displayed in figure C.1. Of the belts tested, sample B (shown in figure C.2) is the one most similar to the belt in the dryer in terms of the opening ratio, having an opening ratio of 0.33. Using linear extrapolation, it is found that pressure drop through sample B is 15 Pa or higher for a velocity of 1.3 m/s. However, as

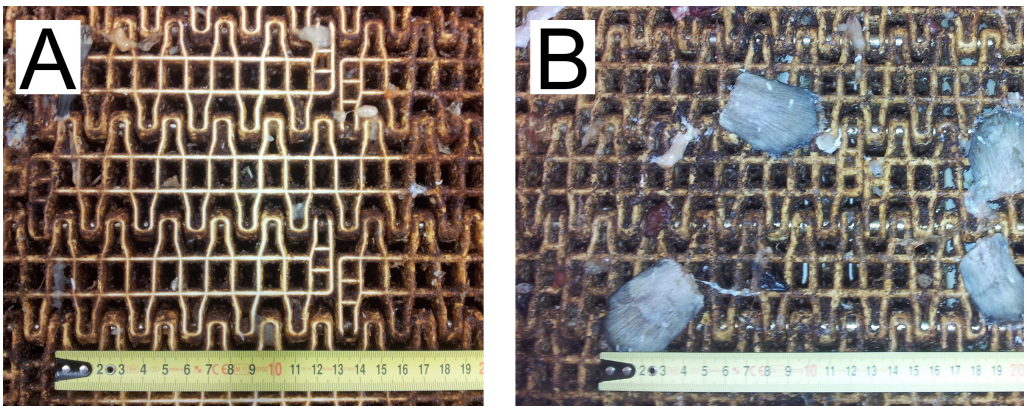


*Figure 4.5: Two samples of conveyor belt inside the dryer.*

mentioned before, opening ratio of the belts in the dryer has been significantly reduced by product residuals so the actual pressure drop is assumably higher still.

Belts of the dryer run in circles inside the dryer so the air must pass twice through each belt on its way through the dryer, for a total of ten passes. Assuming that the same volume of air flows through each belt (no air bypasses the belts or is lost out of the dryer), the pressure drop should be the same through every belt. As a result, actual pressure drop through belts should be in the range of 150 to 250 Pascals. This is a conservative estimate, but it makes up a large part of the total measured pressure drop nevertheless.

The product bed is another factor that affects pressure drop inside the dryer. It is possible to calculate an estimate of pressure drop through the product bed using the Ergun equation (2.11). First, parameters of the equation have to be evaluated along with their associated uncertainty. Dynamic viscosity and density of the air are looked up in CoolProp, assuming the air has a temperature of 27 °C, a pressure of 101.3 kPa and a relative humidity of 60%. Variability of these two parameters is not high within the limits of possible airflow conditions and will not critically affect the outcome. As drying progresses physical properties of the product change so that it will not be packed as densely. Thickness of the product bed is measured with a measurement tape to an certainity within 5 cm. For the lack of a better method, void fraction of the product bed must be estimated visually, which involves a high level of uncertainty. The product is modeled as a plate of length 50 cm and width 10 cm with a uniform thickness of 2 cm. Parameters needed for the calculation are shown in table 4.2.

Because the void fraction can not be known with the same accuracy as other parameters of the Ergun equation, calculated pressure drop through the product bed on each belt is plotted as a function of its void fraction in figure D.1 to explain

*Table 4.2: Parameters used for calculating pressure drop using the Ergun equation.*

| Parameter | Symbol | Value | Unit |
|---|---|---|---|
| Superficial velocity | $v$ | 1.3 | $\mathrm{m/s}$ |
| Dynamic viscosity or air | $\mu$ | $1.842 \times 10^{-5}$ | $\mathrm{kg/(m \cdot s)}$ |
| Density of air | $\rho$ | 1.15 | $\mathrm{kg/m^3}$ |
| Particle surface area | $S_p$ | 0.124 | $\mathrm{m^2}$ |
| Particle volume | $V$ | $1 \times 10^{-3}$ | $\mathrm{m^3}$ |
| Particle specific surface | $a_v$ | 124 | $1/\mathrm{m}$ |
| Effective particle diameter | $D_p$ | $4.8 \times 10^{-2}$ | m |

its potential influence on the results. Table 4.3 shows the measured depth of the product bed on each belt, along with its estimated void fraction and the calculated pressure drop. The combined pressure drop through the product bed of all five belts amounts to 1361 Pa.

*Table 4.3: Measured depth and estimated void fraction of the product bed, along with pressure drop results.*

| Belt | 1 | 2 | 3 | 4 | 5 |
|---|---|---|---|---|---|
| Bed depth (m) | 0.15 | 0.20 | 0.25 | 0.60 | 0.80 |
| Bed void fraction | 0.30 | 0.35 | 0.35 | 0.45 | 0.45 |
| Pressure drop (Pa) | 284 | 215 | 269 | 254 | 339 |

The evaluated pressure drop through the belt and the product bed combined is considerably higher than the measured pressure drop. Observations suggest that that too much air passes through gaps at the end of the belts, instead of passing through the belts. This, along the with the fact of low blower efficiency shows that by reducing the gaps, more air would be forced through the belts, raising the pressure drop along the the efficiency of the blowers. However, this may or may not increase the drying efficency, so an alternative solution might be make no change to the gaps but instead install smaller blowers which would operate at higher efficiency for the current airflow. Having an optimal blower efficiency of 80% for the current airflow, instead of 50%, would drop energy consumption of the blowers by more than 30%.

## 4.2. Temperature and humidity

Measurements of temperature and relative humidity have shown an inconstant state of those variables across the dryer. Shown in figure 4.6 is a two minute long measurement from zone 1, which illustrates an extreme example. In this case, relative humidity fluctuates between 46 and 58% while temperature has a

downward trend from 16 to 12 °C. The cause for this variability is believed to be gusts of wind hitting the building, causing an imbalance in mixing of fresh and recycled air. Conditions of the drying air have a high impact on the drying process and so it stands to reason that knowledge of these conditions is important.

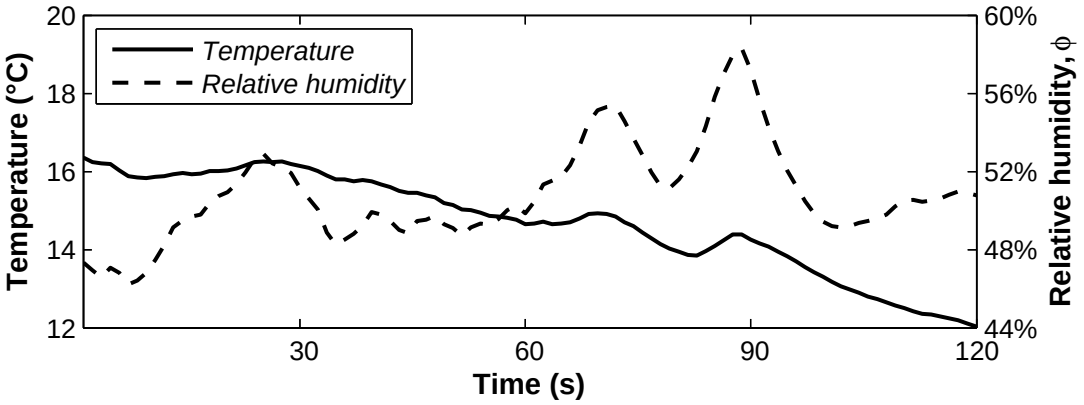


*Figure 4.6: Sample of a temperature and humidity measurements from zone 1.*

Inside the blower compartment, there is a significant temperature difference across the room. Measurements of temperature and relative humidity of the air at the suction inlet of each blower, along with the related specific humidity, is shown in figure 4.7. Nonuniform conditions is not an issue in itself, for any differences will even out inside the dryer. On the other hand, this may be a sign of inadequate insulation and in fact there is an uninsulated door between the outside and the colder end of the blower compartment.

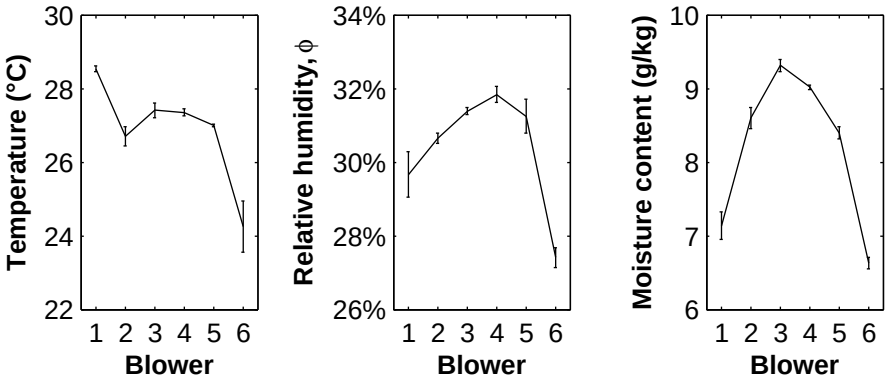


*Figure 4.7: Blower suction temperature and humidity.*

Measurements of temperature and relative humidity from accessible zones in the dryer are presented with a box plot in figure 4.8 to express uncertainity of the measurements. The airflow process can be presented visually by drawing medians of these measurements onto a Mollier chart as shown in figure 4.9. There are two practical reasons for why this process can not have basis in reality. First

reason is that the specific humidity should not be increased during heating of the air, between zones 1 and 2. Secondly, enthalpy of air does not increase during drying, between zones 3 and 5.

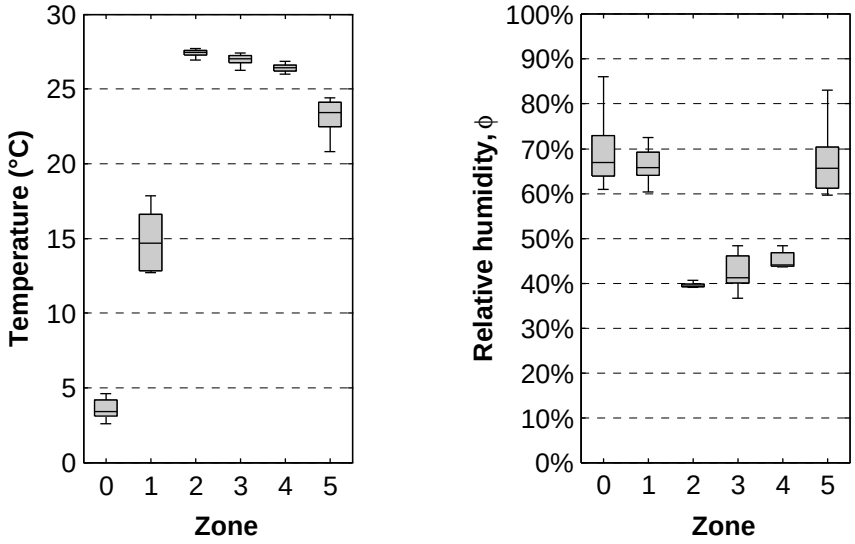


*Figure 4.8: Temperature and humidity measurements. Center line on each box indicates median value and edges of boxes mark 25th and 75th percentiles. Extreme values, excluding outliers, are represented by extended threads.*

There are specific arguments that justify corrections being made to the process diagram, so that it can describe the process more realistically. Only a relatively small shift in one varible can affect the results significantly, but measurements are not taken simultaneously while variability of individual measurements is high. Points 2, 3, 4 and 5 all lie close to a single isenthalpic line but specific humidity in points 1 and 2 should be the same (represented by a vertical line), which suggests that point 1 is incorrect. Comparison of figures 4.8 and 4.9 shows that within quartiles of measurements from zones 1 and 5 can be found values that fulfill a realistic process. The corrected process diagram is shown in figure 4.10.

Examination of temperature and humidity measurements shows that the drying conditions are mostly within a desired range. Measured temperature of the air entering the dryer is close to 28 °C, which is above the preferred temperature of 25 °C but not above a critical value for fishbone (Arason, 2011). The air exiting the dryer is measured to have a temperature of 22 °C and a relative humidity of 67%, which indicates that there is room for improving efficiency because product enters the dryer at 5 °C and is only heated to 16 °C on the top belt.

Results from measurements of the airflow conditions can be used to evaluate some properties of the dryer. The recycling ratio is found to be $41.8^{+27.5}_{-19.0}$% but for the instance shown in figure 4.10, it is found to be 63.6%, which is an unusually high

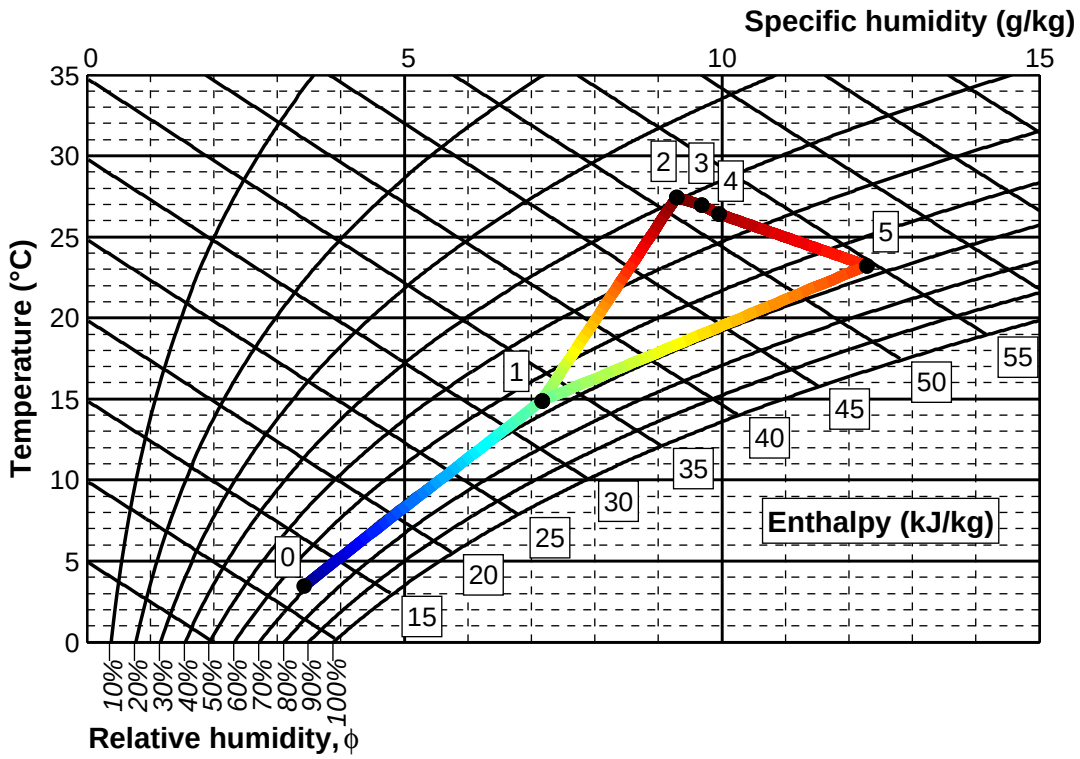


*Figure 4.9: Mollier diagram showing the airflow process using median values. Color of the line represents temperature.*

recycle ratio (Arason, 2011). The rate of heat supply through the heat exchanger is found using equation (2.7), where density and specific heat capacity of the air are taken to be the average of that in zones 1 and 2. Using quartiles of each varible for tolerance, it is found that $q_H = 985 \pm 183\,\text{kW}$, but for the scenario in figure 4.10 it is 919 kW. Adiabatic efficiency is calculated using equation (2.10) and is found to be 50.5%. This means that the maximum usable heat that goes towards evaporating moisture is $497 \pm 92\,\text{kW}$.

Finally, the temperature and humidity measurements also provide an opportunity to evalutate the rate at which moisture is removed from the dryer.

$$\dot{m}_{evap} = G(Y_5 - Y_3)$$

$$= 602\,\text{kg/h}$$

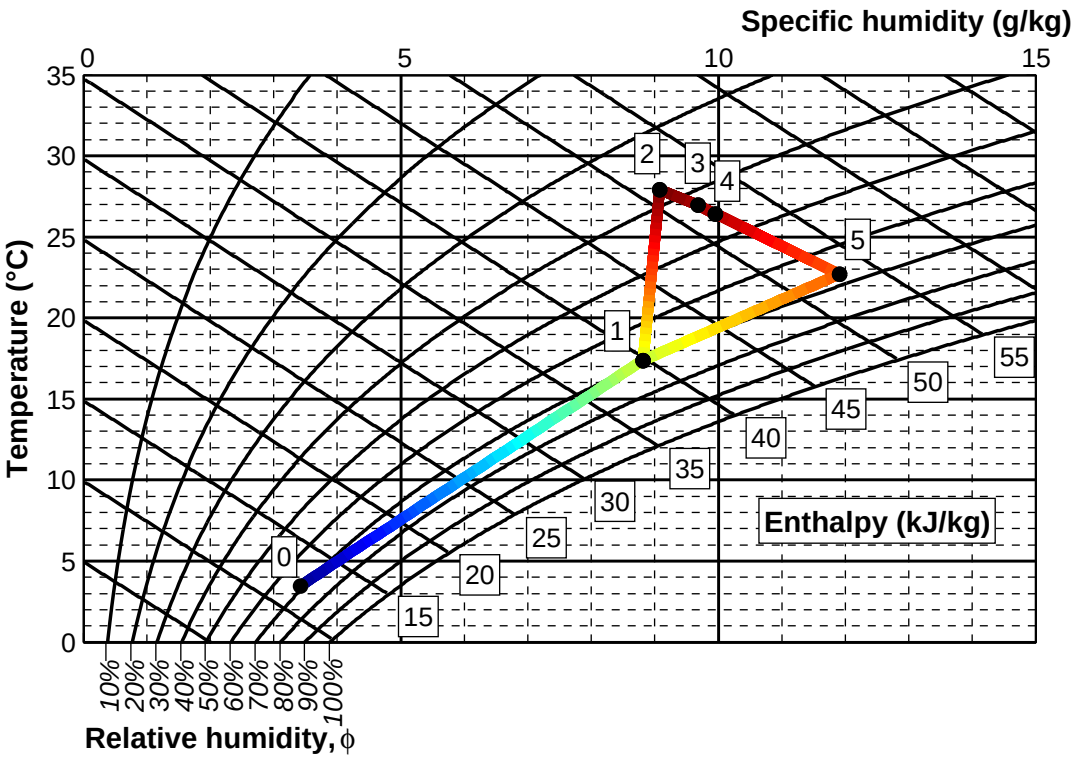


*Figure 4.10: Corrected Mollier diagram showing the airflow process using values within quartile tolerances.*

## 4.3. Product flow

In order to perform general analysis of the overall drying process, there is no need for more information than the airflow conditions in four locations (zones 0, 1, 2 and 5) along with inlet and discharge product moisture content. However, to gain further insight into the process, measurements from intermediate stages are needed. There is only one relevant intermediate airflow measurement is available, from zone 4, which can be used to find out how much water the airflow gains from the bottom two and top three conveyors respectively. Measuring moisture content of the product at intermediate stages can be used to fill in the blanks where airflow measurements are not available.

When the dryer cycles, the whole product bed cascades all at once from one belt to the one beneath, except for the bottom two belts which run slower than the top three. For this reason, it is sufficient to collect product samples from each end of every belt. Results of moisture content measurements are shown in table 4.4 and they indicate that the product is remarkably dry when it leaves the dryer. At the end of primary drying, the product contains even less moisture than the finished

product is supposed to after secondary drying. This means that the production capacity and efficiency of the conveyor dryer is reduced, all energy used during secondary drying is wasted and in the end there may be product giveaway. The goal of primary drying is to efficiently remove moisture during the period of constant drying rate.

*Table 4.4: Results of product moisture content measurements at 6 different stages in primary drying.*

| **Belt** | **1** | **2** | **3** | **4** | **5** |
|---|---|---|---|---|---|
| Prdocut infeed moisture content (%wwb) | 78.0 | 66.0 | 53.3 | 36.2 | 15.5 |
| Product discharge moisture content (%wwb) | 66.0 | 53.3 | 36.2 | 15.5 | 11.0 |

In order to model moisture content and drying rate of the product, it is essential to know the accumulated retention time of the product samples. To make an independent assessment of the drying time, the rate of evaporation (which has been estimated through measurements of the airflow to be 602 kg/h in a previous section), will be matched to the measured moisture loss of the product. This method will assume that the dryer is used continuosly and that the relative speed of the belts will stay constant.

To find the absolute amount of moisture removed from the product on each belt, the weight of the initial product bed must be estimated. This is done by finding the volume of the bed on the top belt, and weighing a sample of fresh product to estimate its initial bulk density. The belts are measured to be 2.8 m wide and 18.1 m long, having a total area of 50.7 $m^2$. Thickness of the top bed is 0.15 m and its bulk density is found to be 500 $kg/m^3$. Weight of the top bed is thus 3800 kg. Using results of moisture content measurements, the amount of water evaporated from each belt is found. Using the rate of evaporation along with the relative speed of the belts, the total drying time is found to be 42.0 hours. The evaluated retention time of each belt is shown in table 4.5.

*Table 4.5: Equivalent retention time of each belt, assuming a total drying time of 30 hours.*

| **Belt** | **1** | **2** | **3** | **4** | **5** |
|---|---|---|---|---|---|
| Relative speed of belt (-) | 1.0 | 1.0 | 1.0 | 0.4 | 0.3 |
| Evaluated retention time (h) | 4.8 | 4.8 | 4.8 | 11.8 | 15.8 |
| Cumulative retention time (h) | 4.8 | 9.6 | 14.4 | 26.2 | 42.0 |

Using the moisture content measurements and the equivalent retention time, a drying curve is fitted with the logarithmic function (2.1), by method of non-linear least squares with a trust region algorithm (MATLAB, 2014; Venkataraman, 2009). The fit is good, but it is worth noting that quality of fit may be relative using so few points. The drying curves are plotted in figure 4.11 and they show that moisture content of fishbone is in the range of 45-55%wwb at the point where

period of falling drying rate begins and primary drying should end. Retention time in primary drying can thus be shortened proportionally. These results also provide and explanation for why so much air is recycled. The rate of evaporation is so low that a large portion of the exhaust air must be recycled to maintain the necessary relative humidity in zone 3 (40%). A closer look will be taken at product moisture content in the next section.

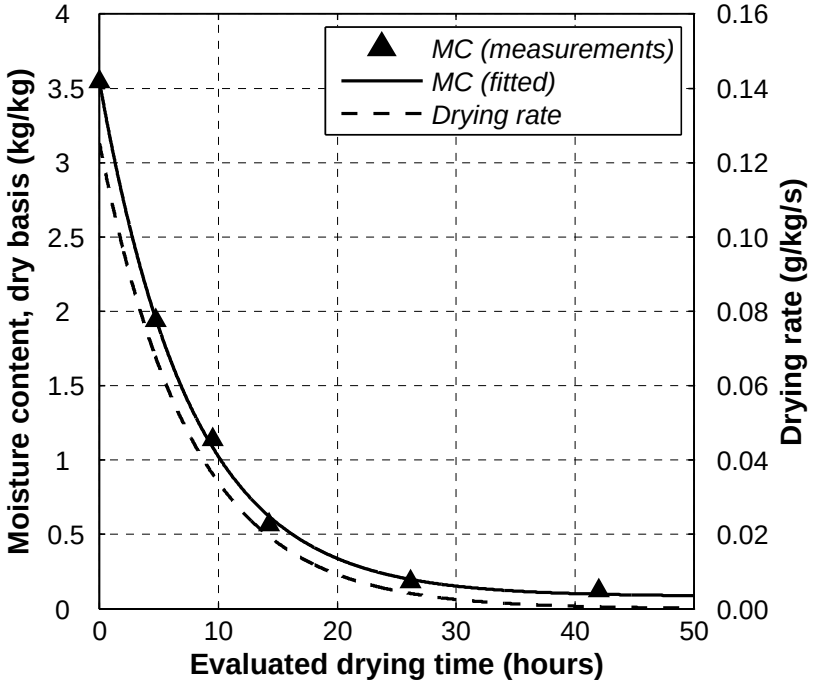


*Figure 4.11: Moisture content (dry basis) and drying rate of fishbone.*

## 4.4. Balance calculations and energy aspects

Calculating heat and mass balances for the drying process is done by creating a model in spreadsheet software. The model involves a heat and a mass balance for water along with a mass balance for the dry ingredients. The balances are calculated in the same way as described in the background chapter, using results from the previous sections. Table 4.6 shows results of balance calculations using measurements of the conveyor dryer where the corrected airflow conditions from figure 4.10 are used.

The model assumes that the heat necessary to evaporate water and heat the vapor to the exhaust temperature is proportional to the change in enthalpy of the water, $\Delta h_w$. The evaporated water enters the dryer in the form of liquid inside the

product at 5 °C ($h_{water} = 21.0$ kJ/kg) and leaves as water vapor at a temperature of at least 23.7 °C ($h_{vapor} = 2544.1$ kJ/kg). Heat to evaporated water is then found by equation (2.6).

*Table 4.6: Dryer balances*

| | **Belt 1** | **Belt 2** | **Belt 3** | **Belt 4** | **Belt 5** | **Total** |
|---|---|---|---|---|---|---|
| Relative speed of belt (-) | 1.0 | 1.0 | 1.0 | 0.4 | 0.3 | |
| Bed depth (m) | 0.15 | 0.20 | 0.25 | 0.6 | 0.8 | |
| Bed area ($m^2$) | 50.7 | 50.7 | 50.7 | 50.7 | 50.7 | 253.4 |
| Evaluated retention time (h) | 4.8 | 4.8 | 4.8 | 11.8 | 15.8 | 42.0 |
| Airflow ($m^3$/h) | 65.6 | 65.6 | 65.6 | 65.6 | 65.6 | |
| Product infeed (kg/h) | 800 | 517.6 | 376.9 | 275.9 | 208.3 | |
| Product infeed moisture (%wwb) | 78.0 | 66.0 | 53.3 | 36.2 | 15.5 | |
| Product discharge (kg/h) | 517.6 | 376.9 | 275.9 | 208.3 | 197.8 | |
| Product discharge moisture (%wwb) | 66.0 | 53.3 | 36.2 | 15.5 | 11.0 | |
| Evaporation (kg/h) | 282.4 | 140.8 | 101.0 | 67.6 | 10.5 | 602.2 |
| Product infeed temperature (°C) | 5 | 17 | 20 | 23 | 26 | |
| Product discharge temperature (°C) | 17 | 20 | 23 | 26 | 29 | |
| Air temperature into bed (°C) | — | — | 26.4 | — | 27.0 | |
| Air temperature out of bed (°C) | 22.7 | — | — | 26.4 | — | |
| Humidity into bed (%RH) | — | — | 45.0 | — | 42.4 | |
| Humidity out of bed (%RH) | 67.0 | — | — | 45.0 | — | |
| Specific humidity into bed (g/kg) | — | — | 9.9 | — | 9.7 | |
| Specific humidity out of bed (g/kg) | 11.9 | — | — | 9.9 | — | |
| Heat to product (kW) | 0.8 | 0.2 | 0.2 | 0.2 | 0.2 | 1.6 |
| Heat to evaporated water (kW) | 198 | 99 | 71 | 47 | 7 | 422 |

The balances in table 4.6 show that the amount of heat to product is clearly a negligible portion of the total heat consumption in comparison to the heat to evaporation. Using product retention times and averages of the product infeed and dischage rates of each belt, it is estimated that the dryer holds 12.9 tonnes of wet product when it is in full operation.

The proportional difference in rate of evaporation between the top three belts and the bottom two belts can be calculated using the change in specific humidity of the air and also from the product moisture content. Using measurements of the specific humidity, this proportional difference is found to be

$$\frac{Y_5 - Y_4}{Y_4 - Y_3} = 7.2$$

Using the rate of evaporation from table 4.6, the ratio is found to be 6.7. This gives a sense of how much more water is evaporated from the product on the top three belts than from the bottom two, due to the difference in drying rate. It is worth noting the difference in this result, which depends on which measurement source is used.

Results from the balance calculations in table 4.6 show that the heat required to evaporate water at the rate of 602 kg/h is 422 kW. The maximum usable heat towards evaporation was previously found to be 465 kW, so losses constitute 9.3% of the usable heat. The overall energy efficiency of the dryer is

$$\eta_0 = \frac{q_{H,min}}{q_H} = \frac{422\,\text{kW}}{919\,\text{kW}} = 45.9\%$$

and it follows that the energy required for evaporating one kilogram of water from a substance is 5495 kJ (1313 kcal).

A simplified diagram of the utility system is shown in figure 4.12. The utility system consists of a closed loop, using water as medium for heat transfer. Saturated brine enters the heat exchanger at a temperature of 155 °C and a pressure of 3.3 bar but exits at 55 °C and atmospheric pressure ($\Delta h_b = 2541.61$ kJ/kg). Assuming an overall 90% efficiency in the utility system (Arason, 2013), the mass rate of brine is calculated to be 1448 kg/h.

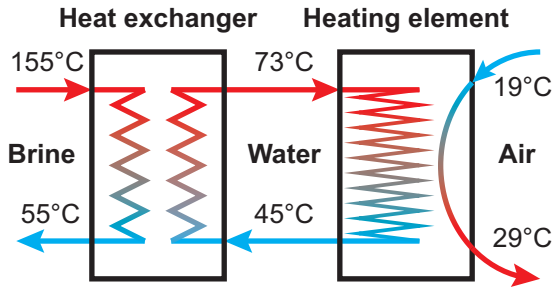


*Figure 4.12: Temperature in the heating system.*

The cost of heating air for drying cod heads and stockfish in cabinet dryers has been published (Arason, 2001; Arason and Árnason, 1992; Arason et al., 1982) and to conclude this chapter, cost of heating air for drying fishbone in a conveyor dryer will be presented. The cost of heating can either be expressed in terms of unit mass final product or in terms of unit mass moisture evaporated from the product. According to measurements of moisture content (table 4.4), 3 kg of water must be evaporated for each kilogram of product exiting the dryer. It follows that the heat needed to produce 1 kg of product by evaporating 3 kg of water is 3939 kcal.

The supply rate of the primary heat source (the geothermal brine) is not measured by Haustak or the power company because the power company charges a fixed fee. For this reason, the supply rate of the primary heat source can not be used to estimate efficiency of the utility system or to check other calculations.

To estimate the cost of heating by using different energy sources, some basic assumtions must be made. The efficiency of oil boilers is estimated at 85% and

coefficient of performance of heat pumps is taken to be 2.5 (Arason, 2001; Green and Perry, 2007). Calorific value of electricity is 860 kcal/kWh and 9300 kcal/litre for marine gas oil similar to No. 2 fuel oil (Green and Perry, 2007). Hot water for heating is cooled from 75 °C to 30 °C, so the calorific value of a hot water energy source is 45 kcal/$m^3$.

The cost of heating air for drying one kilogram of fishbone is shown in figure 4.13, taxes are not included. The results show that the cost of using oil or electricity for heating is considerably higher than the cost of using hot water or geothermal steam.

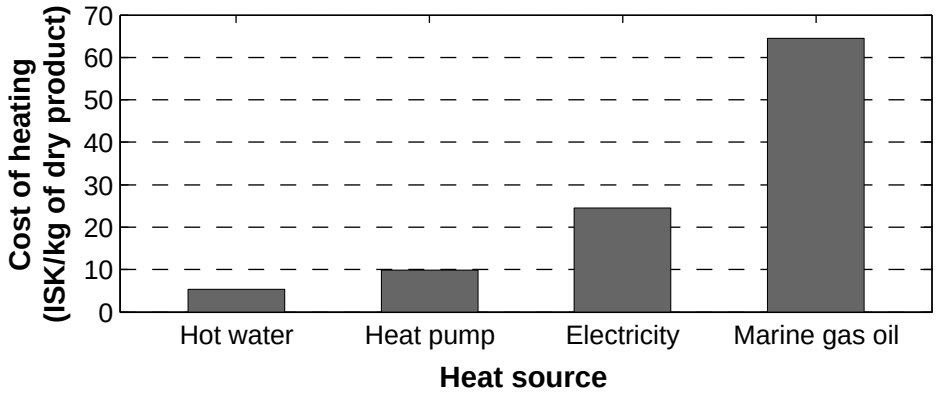


*Figure 4.13: Energy costs of heating air for drying one kilogram of fishbone in a conveyor dryer, in Iceland. Main assumptions are the amount of energy needed to evaporate one kilogram of water from a substance (1313 kcal), efficiency of oil boilers (85%) and coefficient of performance of heat pumps (2.5). Hot water is cooled from* 75 °C *to* 30 °C.

The cost of different energy sources for air drying of fish meal was studied in the early eighties and the cost of using electricity was found to be 66-99% higher than for oil (Jónsson, 1981). Since then, the price of oil has risen and new contracts for the sale of electricity have been made. Today, the cost of electricity is approximately 62% lower than the cost of oil.

# 5. Conclusion

In this study of the latest conveyor dryer in Iceland, measurements of airflow properties and product moisture content have been made and the results used to set up energy balances. The findings show that there are ways to substantially improve effectiveness and efficiency of the dryers operation and design.

Measurements of product moisture content have shown that the product leaving the conveyor dryer is fully dried, at which point it has yet to go through secondary drying. This completely defeats the purpose of dividing the drying process into two stages. Overdrying the product in primary drying results in wasted production capacity and reduced efficiency. This could be avoided by developing process control, e.g. to monitor moisture content of the product leaving the conveyor dryer. Ideally, the dryer should be run continously instead of only being operated in daytime shifts on weekdays. Continous operation of the dryer would contribute towards uniform product quality and a predictable production rate. This might be achived by automatizing some parts of the process, for example the loading and unloading of the dryer. According to results of moisture content measurements (figure 4.11), the current production capacity might be more than doubled if the product is not overdryed.

The primary shortcoming of the design is inadequate efficiency of the airflow which presents itself in a mismatch of measured and calculated pressure drop through the dryer. Gaps at the end of each belt allow a portion of the air to flow in a zigzag pattern through the dryer instead of passing through the perforated belts as intended. The blowers installed in the dryer operate at reduced efficiency in these conditions. The proposed action to increase airflow efficiency is to reduce or close the gaps and use belts with a higher opening ratio; this would force more air to pass through the product bed. If unsuccessful, an alternate action may be to install blowers of lower capacity, which would operate at higher efficiency. To facilitate airflow through the belts, the design should allow easy access for regular cleaning.In order to reduce fluctuations in the mixing of recycled and fresh air, it is advisable to install a simple diffuser mechanism at the fresh air inlet. Finally, improved instrumentation would lead to better overview and control of the process, for example by measuring state of the airflow between each set of belts. By placing load cells under the belts, the product bed could be continously weighed in order to monitor evaporation from each belt and prevent overdrying.

The results include some key operational figures of the dryer and a summary is shown in table 5.1. Nearly 64% of the exhaust air is recycled to regulate relative humidity of the air entering the dryer. A high recycle ratio lifts the adiabatic efficiency, but the cool ambient air lowers it. The energy needed to evaporate each kilogram of water from the product is found to be 1.313 kcal. Comparing these results to the documented performance of cabinet dryers in drying of codheads (Arason, 2001; Arason and Árnason, 1992; Arason et al., 1982) shows inferiority of the conveyor dryer in terms of efficiency. This is the consequence of airflow inefficiency and overdrying.

*Table 5.1: Key operational figures of the dryer*

| | | |
|---|---|---|
| Recycling ratio | $r$ | 63.6% |
| Rate of heat supply | $q_H$ | 919 kW |
| Adiabatic efficiency | $\eta$ | 50.5% |
| Maximum usable heat | $\eta q_H$ | 465 kW |
| Rate of evaporation | $\dot{m}_{evap}$ | 602 kg/h |
| Heat towards evaporation | $q_{H,min}$ | 422 kW |
| Losses | $Q_{loss}$ | 43 kW |
| Overall energy efficiency | $\eta_0$ | 45.9% |

This study answers fundamental questions about the dryer, but there is no doubt that further research into the subject would be of additional benefit. To begin with, it would be recommendable to rectify the problems that have already been pointed out, repeat a similar study and assess improvement. The conveyor dryer is capable of drying various types of product other than fishbone and it would be practical to map the drying curves for other products as well. To further improve knowledge of the airflow charateristics, pressure drop through the dryer should be measured for a variable flow rate of air, both in a empty dryer and a during normal operation. The operators of the dryer have been appreciative of its effectiveness so far, but the conveyor dryer is not perfect and no part of it should be exempt from scrutiny. It has already been shown that there are ways to improve the dryer and a combination of these suggested researches would add up to a comprehensive guide for further development of the equipment.

# References


S. Arason. Nýting jarðvarma í fiskiðnaði. In *Orkuþing 2001: Orkumenning á Íslandi*, pages 135--146. Samorka, October 2001. URL `http://www.samorka.is/doc/1041`. Accessed: Sep 27 2014.

S. Arason. Lecture notes in fish industry technology 1 (VÉL502M). University of Iceland, Reykjavik, 2011.

S. Arason and H. Árnason. Utilization of geothermal energy for drying fish products. *Geothermics*, 21, 1992.

S. Arason, Þ. Jónsson, and T. Þ. Þorsteinsson. Nokkur almenn atriði um úti- og inniþurrkun bolfisks. *Tæknitíðindi*, 136, 1982. URL `http://www.matis.is/media/utgafa//Taeknitidindi136.pdf`. Accessed: Sep 27 2014.

Sigurjón Arason. personal communication, May 29 2013.

Atmel Corporation. ATmega328 data sheet, February 2013. URL `http://www.atmel.com/Images/doc8161.pdf`. Rev. 8161D–AVR–10/09.

I.H. Bell, J. Wronski, S. Quoilin, and V. Lemort. Pure and Pseudo-pure Fluid Thermophysical Property Evaluation and the Open-Source Thermophysical Property Library CoolProp. *Industrial & Engineering Chemistry Research*, 53 (6):2498--2508, 2014. URL `http://pubs.acs.org/doi/abs/10.1021/ie4033999`. Accessed: Sep 27 2014.

C.N. Boeri, F.J. Neto da Silva, J.A.F. Ferreira, J.M.A. Saraiva, and R.S. Moreira. Equilibrium moisture content isotherms of codfish (gadus morhua). *Journal of Aquatic Food Product Technology*, 22(6):551--563, 2013.

Bosch Sensortec. BMP180 Digital pressure sensor data sheet, Rev. 2.5., April 2013. URL `http://dlnmh9ip6v2uc.cloudfront.net/datasheets/Sensors/Pressure/BMP180.pdf`. Accessed: Sep 27 2014.

D.M. Bruce. Exposed-layer barley drying: three models fitted to new data up to 150 c. *Journal of Agricultural Engineering Research*, 32(4):337--348, 1985.

X.D. Chen and A.S. Mujumdar. *Drying Technologies in Food Processing*. Wiley, 2009.

L.M. Diamante and P.A. Munro. Mathematical modelling of hot air drying of sweet potato slices. *International journal of food science & technology*, 26(1):99--109, 1991.

Digi International. XBee Product Manual, February 2014. URL `http://ftp1.digi.com/support/documentation/90000982_P.pdf`. v1.xEx.

Dynair. PR-L Blower Catalogue, May 2014. URL `http://dynair.it/upload/allegatiprodotti/PR-L.DYN533d16969afd0.pdf`. Accessed: Sep 27 2014.

S. Ergun. Fluid flow through packed columns. *Chem. Eng. Prog.*, 48:89--94, 1952.

D. Green and R. Perry. *Perry's Chemical Engineers' Handbook, Eighth Edition*. McGraw Hill professional. McGraw-Hill Education, 2007.

B. Hallström, C. Skjöldebrand, and C. Trägårdh. *Heat transfer and food products*. London ; New York : Elsevier Applied Science, 1988.

S.M. Henderson. Progress in developing the thin layer drying equation [for maize]. *Transactions of the ASAE (USA)*, 1974.

S.M. Henderson and S. Pabis. Grain drying theory i. temperature effect on drying coefficient. *Journal of Agricultural Engineering Research*, 6(3):169--174, 1961.

J.P. Holman. *Heat Transfer*. McGraw-Hill series in mechanical engineering. McGraw Hill Higher Education, 2010.

Þ. Jónsson. Electric drying of fish meal, 1981. Reykjavik: Mechanical engineering, University of Iceland.

R.B. Keey. *Drying principles and practice*. International series of monographs in chemical engineering. Pergamon Press, 1972.

R.B. Keey. *Drying Of Loose And Particulate Materials*. Taylor & Francis, 1991.

I.C. Kemp. *Fundamentals of energy analysis of dryers*. Wiley-VCH: Weinheim, Germany, 2012.

I.C. Kemp and S.P. Gardiner. An outline method for troubleshooting and problem-solving in dryers. *Drying Technology*, 19(8):1875--1890, 2001.

T.L. Lai, H. Robbins, and C.Z. Wei. Strong consistency of least squares estimates in multiple regression. In *Herbert Robbins Selected Papers*, pages 510--512. Springer, 1985.

M. Leva, M. Weintraub, M. Grummer, M. Pollchik, and H.H. Storch. *Fluid flow through packed and fluidized systems*. US Government Printing Office, 1951.

W. K. Lewis. The rate of drying of solid materials. *Industrial & Engineering Chemistry*, 13, May 1921.

MATLAB. *MATLAB Version 8.3.0.532 (R2014a) Documentation*. The MathWorks Inc., Natick, Massachusetts, 2014. URL `http://www.mathworks.se/help/matlab/`. Accessed: Sep 27 2014.

A.S. Mujumdar. Principles, classicication, and selection of dryers. In A.S. Mujumdar, editor, *Handbook of Industrial Drying*. Taylor & Francis, 2006.

NXP Semiconductors. $I^2C$-bus specification and user manual, April 2014. URL `http://www.nxp.com/documents/user_manual/UM10204.pdf`. Rev. 6.

G.E. Page. Factors influencing the maximum rates of air drying shelled corn in thin layers, 1949. URL `http://docs.lib.purdue.edu/dissertations/AAI1300089/`. Accessed: Sep 27 2014.

D. Poirier. Conveyor dryers. In A.S. Mujumdar, editor, *Handbook of Industrial Drying*. Taylor & Francis, 2006.

M.M. Prado and D.J.M. Sartori. Simultaneous heat and mass transfer in packed bed brying of seeds having a mucilage coating. *Brazilian Journal of Chemical Engineering*, 25(1):39--50, 2008.

M.M. Prado and D.J.M. Sartori. Heat and mass transfer in packed bed drying of shrinking particles. In Prof. Mohamed El-Amin (Ed.), editor, *Mass Transfer in Multiphase Systems and its Applications*. InTech, 2011. URL `http://www.intechopen.com/books/mass-transfer-in-multiphase-systems-and-its-applications/heat-and-mass-transfer-in-packed-bed-drying-of-shrinking-particles`. Accessed: Sep 27 2014.

M.S. Rahman. Drying of fish and seafood. In A.S. Mujumdar, editor, *Handbook of Industrial Drying*. Taylor & Francis, 2006.

S. Rahman. *Handbook of Food Preservation, Second Edition*. Food Science and Technology. Taylor & Francis, 2007.

P. Rakesh. AC Induction motor fundamentals, 2003. URL `http://ww1.microchip.com/downloads/en/AppNotes/00887a.pdf`. Accessed: Sep 27 2014.

Sensirion. SHT15 Calibration Certification, August 2010. URL `http://www.sensirion.com/fileadmin/user_upload/customers/sensirion/Dokumente/Humidity/Sensirion_Humidity_SHTxx_Calibration_Certification.pdf`. Accessed: Sep 27 2014.

Sensirion. SHT15 Digital pressure sensor data sheet, Rev. 5, December 2011. URL `http://www.sensirion.com/fileadmin/user_upload/customers/sensirion/Dokumente/Humidity/Sensirion_Humidity_SHT1x_Datasheet_V5.pdf`. Accessed: Sep 27 2014.

B. Sivasankar. *Food Processing and Preservation*. PHI Learning, 2002.

Statistics Iceland. Export of marine products, April 2014. URL `http://www.statice.is/Statistics/Fisheries-and-agriculture/Export`. Accessed: Sep 27 2014.

Testo AG. Testo 452 Instruction Manual, N.d. URL `http://www.testo.fr/resources/media/global_media/produkte/testo_452/452_IM_0971_1380_0192.pdf`. Accessed: Sep 27 2014.

İ.T. Toğrul and D. Pehlivan. Mathematical modelling of solar drying of apricots in thin layers. *Journal of Food Engineering*, 55(3):209--216, 2002.

W.B. Van Arsdel, M.J. Copley, and A.I. Morgan. *Food dehydration: Drying methods and phenomena*. Food Dehydration. Avi Pub. Co., 1973.

P. Venkataraman. *Applied Optimization with MATLAB Programming*. Wiley, 2009.

C.Y. Wang and R.P. Singh. Use of variable equilibrium moisture content in modeling rice drying. *Transactions of American Society of Agricultural Engineers*, 11(6):668--672, 1978.

F.M. White. *Fluid Mechanics*. McGraw-Hill series in mechanical engineering. McGraw-Hill, 2011.

G.M. White, I.J. Ross, and C.G. Poneleit. Fully-exposed drying of popcorn. *Transactions of the ASAE [American Society of Agricultural Engineers]*, 1981.

P. Zeuthen and L. Bøgh-Sørensen. *Food Preservation Techniques*. Woodhead Publishing series in food science and technology. Woodhead Publ., 2003.

# A. Measuring equipment

For measuring relative humidity a SHT15 digital humidity sensor manufactured by Sensirion is chosen. According to specifications, the sensor offers a absolute relative humiditiy measurement range of 0-100%RH with accuracy of $\pm$2% in the range of 10-90%RH and a repeatability of $\pm$0.1%RH (Sensirion, 2011). The sensor comes with a calibration certificate, so a simple check is determined satisfactory to verify the functionality of the sensor (Sensirion, 2010). A check is conducted by measuring relative humidity of air above a saturated solution of barium chloride ($BaCl_2$), which has a water activity of 0.902 at 25°C (Sivasankar, 2002). One hour measurement with the sensor shows a relative humidity of 90.7% with a standard deviation of 0.2% at a termperature of 23.7°C, which is acceptible accuracy for purpose of this study.

To measure absolute air pressure, a high precision digital barometric pressure sensor, model BMP180 by Bosch, is selected. Pressure measuring range is 300 to 1100 hPa with an accuracy down to 2 Pa due to low noise and with help of a finite impulse response filter. Calibration parameters are stored in read-only memory by the manufacturer, but no certificate of calibration is supplied (Bosch Sensortec, 2013). The calibration of the sensor is therefore verified at the Icelandic Meteorological Office by placing the sensor inside a slightly pressurized vessel along with a certified ultra-accurate pressure measurement device (see figure A.1).

*Figure A.1: Pressure sensor calibration at the Icelandic Meteorological Office.*

In order to calibrate the pressure sensor, 60 instantaneous readings are made for 18 different values of pressure in the range of 1045-1057 hPa (see figure A.2).

Applying a linear regression to the measurements with method of ordinary least squares shows that the sensor has an internal error of 0.03% and offset of 80 Pa (Lai et al., 1985). This error is deemed acceptible for measuring pressure differences of less than 1 kPa.

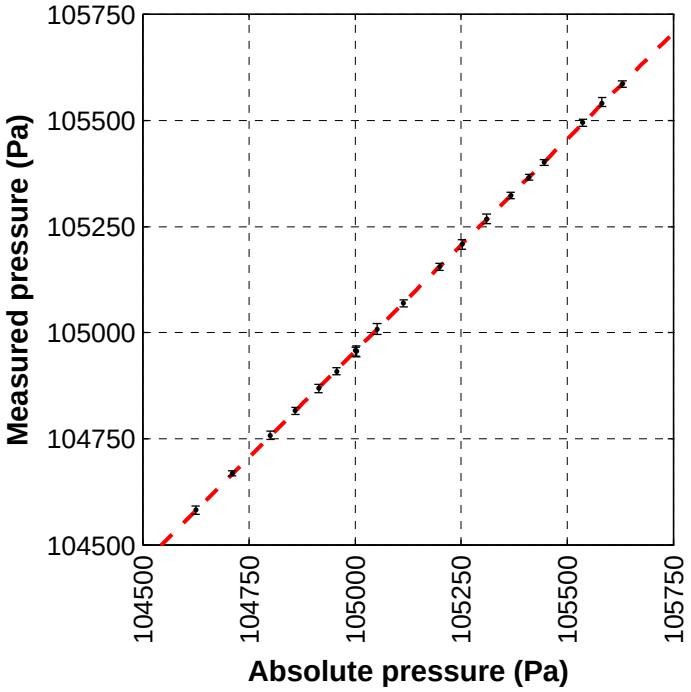


*Figure A.2: Pressure sensor calibration results.*

$$P_{measured} = \frac{2871}{2870} \cdot P_{actual} - 80\text{Pa}$$

Both sensors also include an auxiliary temperature sensor which are utilized. No calibration of temperature sensors is performed, but it is worth noting that the SHT15 calibration certificate is also valid for its temperature sensor and that the temperature sensor of the BMP180 consistently gives a 0.1°C lower reading. This suggests that there may be no need for detailed calibration of the temperature sensors.

Measurements are read from the sensors using a microprocessor development board called Arduino UNO, but the board is based around a microcontroller model ATmega328 from Atmel AVR (Atmel Corporation, 2013). The board reads data from the sensors over a two wire serial interface, which is an implementation of an inter-integrated circuit (I²C) bus (NXP Semiconductors, 2014). A program for the board, written in C/C++, can be found in appendix B.

For increased flexibility, the device is battery powered and connected wirelessly

to a portable computer which initiates measurements and collect measurement data in real time. For this purpose, a couple of XBee wireless modems are used, model XB24-AWI manufactured by Digi International. These modems use an IEEE 802.15.4 standard at a frequency of 2.4GHz and can be used to forward serial communication at data rate up to 250kbps (Digi International, 2014).

*Figure A.3: Measurement device.*

# B. Code

## main.m - Arduino program

```
1 // This arduino program reads temperature and humidity measurements
2 // from a SHT15 humidity sensor as well as temperature and pressure
3 // measurements from a BMP085 pressure sensor.
4 //
5 // This code is based on snippets from a number of different sources,
6 // please see the links below for further details. Special credit
7 // goes to Jim Lindblom for his BMP085 example code.
8 // http://bildr.org/2012/11/sht15-arduino/
9 // http://wiring.org.co/learning/basics/humiditytemperaturesht15.html
10 // http://www.glacialwanderer.com/hobbyrobotics/?p=5
11 // http://bildr.org/2011/06/bmp085-arduino/
12 // https://github.com/sparkfun/BMP180_Breakout
13 //
14 // Copyright (C) 2013  Magnús Kári Ingvarsson
15 // License: CC BY-SA v4.0 http://creativecommons.org/licenses/by/4.0/
16 // WITHOUT ANY WARRANTY
17
18 #include <Wire.h>
19
20 // HUMIDITY VARIABLES
21 int SHT_clockPin = 3;  // Pin used for clock
22 int SHT_dataPin  = 2;  // Pin used for data
23
24 // PRESSURE VARIABLES
25 #define BMP085_ADDRESS 0x77   // I2C address of BMP085
26 const unsigned char OSS = 3;    // Oversampling Setting
27
28 // Calibration values
29 int ac1, ac2, ac3;
30 unsigned int ac4, ac5, ac6;
31 int b1, b2, mb, mc, md;
32
33 //b5 is calculated using bmp085GetTemperature(...), this variable
34 //is also used in bmp085GetPressure(...) so bmp085GetTemperature(...)
35 //must be called before bmp085GetPressure(...).
36 long b5;
37
38 void setup(){
```

```
39   Serial.begin(9600);    // Open serial at 9600 bps
40   Wire.begin();      // Initialize one-wire communication (I2C)
41   bmp085Calibration();  // Read factory calibration coefficients
42 }
43
44 void loop(){      // **Program main loop**
45   // Humidity readings from SHT15
46   float humtemp = getTemperature(); // Read temperature from SHT15
47   float humidity = getHumidity(); // Read humidity from SHT15
48
49   //Pressure readings from BMP085
50   // GetTemperature(...) MUST be called first...
51   float prestemp = bmp085GetTemperature(bmp085ReadUT());
52   float pressure = bmp085GetPressure(bmp085ReadUP());
53
54   //Print humidity data
55   Serial.print(humtemp);    // Temperature reading from SHT15 (°C)
56   Serial.print(", ");
57   Serial.print(humidity);  // Humidity reading from SHT15 (%RH)
58   Serial.print(", ");
59
60   //Print pressure data
61   Serial.print(prestemp, 2); // Temperature reading from BMP085 (°C)
62   Serial.print(", ");
63   Serial.print(pressure, 0); // Pressure reading from BMP085 (Pa)
64
65   Serial.println();       // Send line break
66   delay(5);          // Wait a moment and get values again.
67 }
68
69 //HUMIDITY CODE
70 float getTemperature(){
71   // Return Temperature in Celsius
72   SHT_sendCommand(B00000011, SHT_dataPin, SHT_clockPin);
73   SHT_waitForResult(SHT_dataPin);
74   int val = SHT_getData(SHT_dataPin, SHT_clockPin);
75   SHT_skipCrc(SHT_dataPin, SHT_clockPin);
76   return (float)val * 0.01 - 40; // Convert to celsius
77 }
78
79 float getHumidity(){
80   //Return  Relative Humidity
81   SHT_sendCommand(B00000101, SHT_dataPin, SHT_clockPin);
82   SHT_waitForResult(SHT_dataPin);
83   int val = SHT_getData(SHT_dataPin, SHT_clockPin);
84   SHT_skipCrc(SHT_dataPin, SHT_clockPin);
85   return -4.0 + 0.0405 * val + -0.0000028 * val * val;
86 }
87
88 void SHT_sendCommand(int command, int dataPin, int clockPin){
89   // Sends a command to the SHT15 sensor
90   // Transmission start:
```

```
91    pinMode(dataPin, OUTPUT);
92    pinMode(clockPin, OUTPUT);
93    digitalWrite(dataPin, HIGH);
94    digitalWrite(clockPin, HIGH);
95    digitalWrite(dataPin, LOW);
96    digitalWrite(clockPin, LOW);
97    digitalWrite(clockPin, HIGH);
98    digitalWrite(dataPin, HIGH);
99    digitalWrite(clockPin, LOW);
100
101   // Shift out the command (the 3 MSB are address and must be 000,
102   // the last 5 bits are the command)
103   shiftOut(dataPin, clockPin, MSBFIRST, command);
104
105   // Verify we get the right ACK
106   digitalWrite(clockPin, HIGH);
107   pinMode(dataPin, INPUT);
108
109   if (digitalRead(dataPin)) Serial.println("ACK error 0");
110   digitalWrite(clockPin, LOW);
111   if (!digitalRead(dataPin)) Serial.println("ACK error 1");
112 }
113
114 void SHT_waitForResult(int dataPin){
115   // Wait for the SHT15 answer (up to 2 seconds)
116   pinMode(dataPin, INPUT);
117   int ack;  // Acknowledgement
118   for (int i = 0; i < 1000; ++i){
119     delay(2);
120     ack = digitalRead(dataPin);
121     if (ack == LOW) break;
122   }
123   if (ack == HIGH) Serial.println("ACK error 2");
124 }
125
126 int SHT_getData(int dataPin, int clockPin){
127   // Get data from the SHT15
128
129   // Get the MSB
130   pinMode(dataPin, INPUT);
131   pinMode(clockPin, OUTPUT);
132   byte MSB = shiftIn(dataPin, clockPin, MSBFIRST);
133
134   // Send the required ACK
135   pinMode(dataPin, OUTPUT);
136   digitalWrite(dataPin, HIGH);
137   digitalWrite(dataPin, LOW);
138   digitalWrite(clockPin, HIGH);
139   digitalWrite(clockPin, LOW);
140
141   // Get the LSB
142   pinMode(dataPin, INPUT);
```

```
143   byte LSB = shiftIn(dataPin, clockPin, MSBFIRST);
144   return ((MSB << 8) | LSB); // Combine MSB and LSB
145 }
146
147 void SHT_skipCrc(int dataPin, int clockPin){
148   // Skip CRC data from the SHTx sensor
149   pinMode(dataPin, OUTPUT);
150   pinMode(clockPin, OUTPUT);
151   digitalWrite(dataPin, HIGH);
152   digitalWrite(clockPin, HIGH);
153   digitalWrite(clockPin, LOW);
154 }
155
156 // PRESSURE CODE
157 void bmp085Calibration()
158 {
159   ac1 = bmp085ReadInt(0xAA);
160   ac2 = bmp085ReadInt(0xAC);
161   ac3 = bmp085ReadInt(0xAE);
162   ac4 = bmp085ReadInt(0xB0);
163   ac5 = bmp085ReadInt(0xB2);
164   ac6 = bmp085ReadInt(0xB4);
165   b1 = bmp085ReadInt(0xB6);
166   b2 = bmp085ReadInt(0xB8);
167   mb = bmp085ReadInt(0xBA);
168   mc = bmp085ReadInt(0xBC);
169   md = bmp085ReadInt(0xBE);
170 }
171
172 // Calculate temperature in degrees celsius
173 float bmp085GetTemperature(unsigned int ut){
174   long x1, x2;
175   x1 = (((long)ut - (long)ac6)*(long)ac5) >> 15;
176   x2 = ((long)mc << 11)/(x1 + md);
177   b5 = x1 + x2;
178   float temp = ((b5 + 8)>>4);
179   temp = temp /10;
180   return temp;
181 }
182
183 // Get pressure. Calibration values must be known.
184 // b5 is required so bmp085GetTemperature() must be called first.
185 // Value returned will be pressure in units of Pa.
186 long bmp085GetPressure(unsigned long up){
187   long x1, x2, x3, b3, b6, p;
188   unsigned long b4, b7;
189   b6 = b5 - 4000;
190   // Calculate B3
191   x1 = (b2 * (b6 * b6)>>12)>>11;
192   x2 = (ac2 * b6)>>11;
193   x3 = x1 + x2;
194   b3 = (((((long)ac1)*4 + x3)<<OSS) + 2)>>2;
```

```
195   // Calculate B4
196   x1 = (ac3 * b6)>>13;
197   x2 = (b1 * ((b6 * b6)>>12))>>16;
198   x3 = ((x1 + x2) + 2)>>2;
199   b4 = (ac4 * (unsigned long)(x3 + 32768))>>15;
200   b7 = ((unsigned long)(up - b3) * (50000>>OSS));
201   if (b7 < 0x80000000)
202     p = (b7<<1)/b4;
203   else
204     p = (b7/b4)<<1;
205   x1 = (p>>8) * (p>>8);
206   x1 = (x1 * 3038)>>16;
207   x2 = (-7357 * p)>>16;
208   p += (x1 + x2 + 3791)>>4;
209   return p;
210 }
211
212 // Read 1 byte from the BMP085 at 'address'
213 char bmp085Read(unsigned char address)
214 {
215   unsigned char data;
216   Wire.beginTransmission(BMP085_ADDRESS);
217   Wire.write(address);
218   Wire.endTransmission();
219   Wire.requestFrom(BMP085_ADDRESS, 1);
220   while(!Wire.available())
221     ;
222   return Wire.read();
223 }
224
225 // Read 2 bytes from the BMP085
226 // First byte will be from 'address'
227 // Second byte will be from 'address'+1
228 int bmp085ReadInt(unsigned char address)
229 {
230   unsigned char msb, lsb;
231   Wire.beginTransmission(BMP085_ADDRESS);
232   Wire.write(address);
233   Wire.endTransmission();
234   Wire.requestFrom(BMP085_ADDRESS, 2);
235   while(Wire.available()<2)
236     ;
237   msb = Wire.read();
238   lsb = Wire.read();
239   return (int) msb<<8 | lsb;
240 }
241
242 // Read the uncompensated temperature value
243 unsigned int bmp085ReadUT(){
244   unsigned int ut;
245   // Write 0x2E into Register 0xF4
246   // This requests a temperature reading
```

```
247   Wire.beginTransmission(BMP085_ADDRESS);
248   Wire.write(0xF4);
249   Wire.write(0x2E);
250   Wire.endTransmission();
251   // Wait at least 4.5ms
252   delay(5);
253   // Read two bytes from registers 0xF6 and 0xF7
254   ut = bmp085ReadInt(0xF6);
255   return ut;
256 }
257
258 // Read the uncompensated pressure value
259 unsigned long bmp085ReadUP(){
260   unsigned char msb, lsb, xlsb;
261   unsigned long up = 0;
262   // Write 0x34+(OSS<<6) into register 0xF4
263   // Request a pressure reading w/ oversampling setting
264   Wire.beginTransmission(BMP085_ADDRESS);
265   Wire.write(0xF4);
266   Wire.write(0x34 + (OSS<<6));
267   Wire.endTransmission();
268   // Wait for conversion, delay time dependent on OSS
269   delay(2 + (3<<OSS));
270   // Read register 0xF6 (MSB), 0xF7 (LSB), and 0xF8 (XLSB)
271   msb = bmp085Read(0xF6);
272   lsb = bmp085Read(0xF7);
273   xlsb = bmp085Read(0xF8);
274   up = (((unsigned long) msb << 16) | ((unsigned long) lsb << 8) |
        (unsigned long) xlsb) >> (8-OSS);
275   return up;
276 }
277
278 void writeRegister(int deviceAddress, byte address, byte val) {
279   Wire.beginTransmission(deviceAddress); // start transmission
280   Wire.write(address);                   // send register address
281   Wire.write(val);                       // send value to write
282   Wire.endTransmission();                // end transmission
283 }
284
285 int readRegister(int deviceAddress, byte address){
286   int v;
287   Wire.beginTransmission(deviceAddress);
288   Wire.write(address);            // Register to read
289   Wire.endTransmission();
290   Wire.requestFrom(deviceAddress, 1);     // Read a byte
291   while(!Wire.available()) {
292     // Wait
293   }
294   v = Wire.read();
295   return v;
296 }
```

# main.m - Matlab primary script

```
%% Main.m - Script for reading data from serial port
%
% This script initializes automatic serial read function and timer
% interrupt for reading data from a serial port. When the script is
% terminated, the serial port must be closed by issuing the following
% commands:
%       stopasync(S);     % Stops asynchronous read
%       fclose(S);        % Closes the serial port
%       delete(S);        % Deletes the serial object
%
%   Copyright (C) 2011  Magnús Kári Ingvarsson
%   License: CC BY v4.0 (http://creativecommons.org/licenses/by/4.0/)
%   WITHOUT ANY WARRANTY

% Define global variables
global A t

% A: matrix that stores measurements
% t: integer that counts number of measurements
% Measurement number "t" is stored in line "t" in matrix A

% Variables initialized
A=zeros(2e6,7); t=1;

% Determine OS
disp('Set serial port address in sourcecode...')
if ispc
    port='COM4';      % set serial port for PC here
elseif ismac
    port='/dev/tty.usbserial-A9007MhQ'; % set serial port for Mac here
elseif isunix
    port='/dev/ttyUSB0';    % set serial port for Unix here
end

% Create serial object by setting port address, baudrate and buffersize
S = serial(port,'BAUD',9600,'InputBufferSize', 5000);
% If needed, a timer function can be used to run periodically, e.g. if
% data needs to be saved.
% S.TimerPeriod = 3600;           % Timer function with period 3600s
% S.TimerFcn = {@script};         % Global variables can be transferred

fopen(S);       % Open serial port
readasync(S);   % Read data from the port asynchronously (if available)

% As soon as a terminator-byte (line-ending) is received, the data at
% the serial port is read using the script "readSerial.m"
S.BytesAvailableFcnMode = 'terminator';
S.BytesAvailableFcn = {@readSerial};
```

## readSerial.m - Matlab callback function

```
%% ReadSerial.m - Callback function for the script main.m. Reads
% available data at the sieral port when a terminator byte is received.

function readSerial(obj,event)
    global A t  % Global variables
    try
      % Read formatted data from the serial port...
        tmp=(fscanf(obj,'%f, %f, %f, %f'))';
        % ... and add it to the bottom of the matrix.
        A(t,:)=[tmp now];
        t=t+1;
    end
end
```

# C. Conveyor belt pressure drop

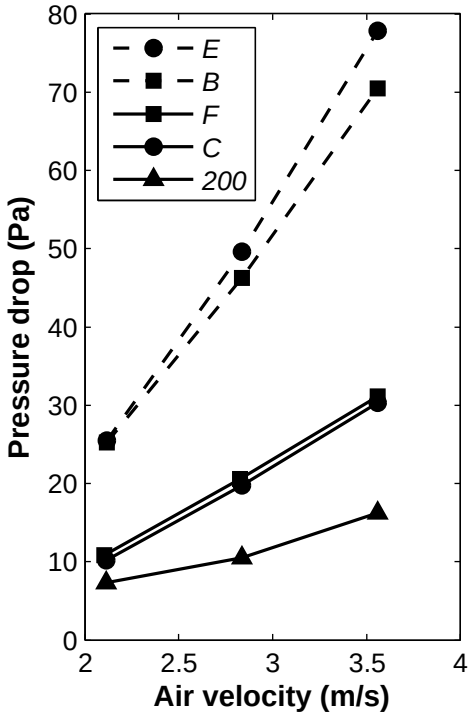


*Figure C.1: Pressure drop through a single thickness of five types of conveyor belts. Test method employed is ANSI/AMCA210-99, ANSI/ASHRAE 51-1999, American national Standard "Laboratory Methods of Testing Fans for rating" . Courtesey of Ashworh Bros., Inc.*

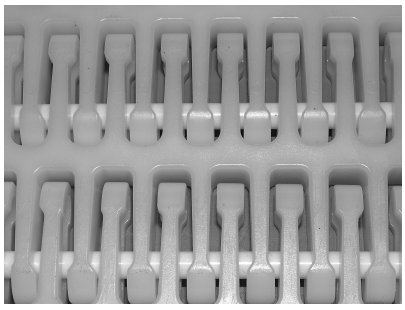

*Figure C.2: Sample B. Courtesey of Ashworh Bros., Inc.*

# D. Evaluation of the Ergun equation

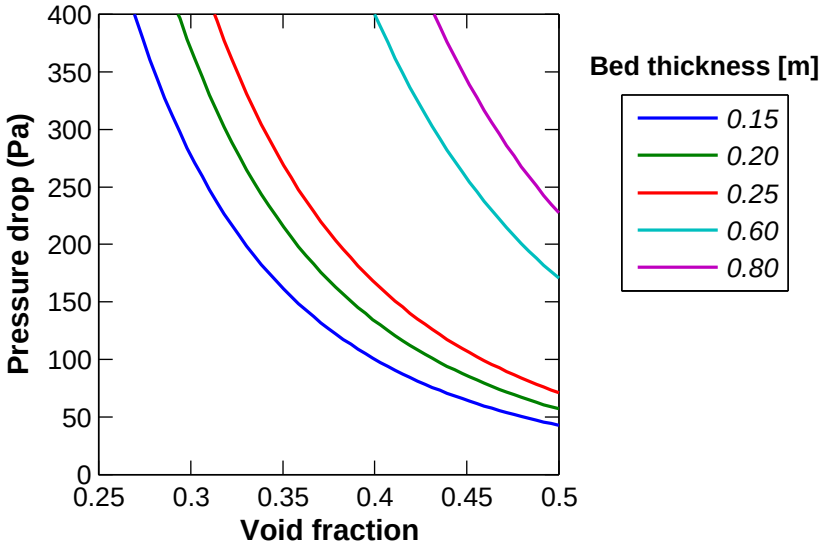


*Figure D.1: Evalutation of pressure drop through the product bed using the Ergun equation with parameters from table 4.2.*